JKAU: Earth Sci., **vol. 11,** pp. 103-141 (1420 A.H. / 1999 A.D.)

Mantle-crustal Source of Mafic-felsic Magmas in the Dubr-Igla Intrusive Complex, Egypt: Inference from Geochemistry and Sr-Nd Isotopic Study

MOHAMED A. HASSANEN
Faculty of Earth Sciences, King Abdulaziz University, Jeddah, Saudi Arabia

Received: 6/4/97 Revised: 7/11/99 Accepted: 6/3/2000

ABSTRACT. The Dubr-Igla intrusive complex (DIC) is a composite batholith intruded into the Pan-African terrain of the Egyptian basement complex. It represents an uplifted tectonic block, comprising a diverse rock association ranging from gabbro to granite. These rocks belong to two distinct suites; the gabbroid-diorite (mafic-intermediate) and granodiorite-monzogranite (felsic) suites. The gabbroid-diorite suite has a calc-alkaline affinity and an overall depletion of Nb, Y, K, and Rb with slightly fractionated REE pattern (La/Yb_n = 0.96 -3.72). The granodiorite and monzogranites are late to post orogenic calc-alkaline rocks with metaluminous to mildly peraluminous character and are relatively enriched in LIL elements but depleted in HFS elements. They have fractionated REE patterns (La/Yb_n =2.62-6.97), flat HREE (Gd/Yb_n = 0.89-1.10) and well-developed negative Eu anomalies (Eu/Eu =0.74-3.0). The granitoid rocks of the DIC have trace element and REE signatures characteristic of I-type granites formed in subduction-related, arc environments.

The whole-rock Rb-Sr isochron ages of the monzogranites and the diorite-quartz diorite from DIC are 644 ± 7 Ma and 704 ± 13 Ma, respectively. The diorite-quartz diorite shows a narrow range of t_{Nd} (+ 6.7 - + 8.5) and initial $^{87}Sr/^{86}Sr$ ratio (0.7022-0.7025). These isotopic characteristics and the overall depletion of the LIL elements and LREE and low Rb/Sr suggest that they had been derived from a depleted mantle source. The granodiorite and monzogranites have low initial $^{87}Sr/^{86}Sri$ ratio (0.7025 - 0.7035) and positive spread t_{Nd}

*Permanent address: Alexandria University, Faculty of Science, Geology Department, Alexandria, Egypt.

(+ 3.4 - + 5.2), which indicate that their protolith was either mantle or most likely juvenile lower crust that had been separated from the mantle.

Isotopic, REE data and numerical modeling performed on the three rock types of the DIC (diorite-quartz diorite, granodiorite and monzogranite) indicate that complex petrogenetic processes generated them as follows: 1) the diorite-quartz diorite was formed by 10%-15% partial melting of mantle-derived basaltic source similar in composition to the associated gabbroid rocks; 2) the monzogranites were derived through: a dehydration melting (30%) of mafic metaigneous lower crustal material due to underplating by a mantle-derived magma which supplies heat budget for melting followed by about 70%-80% fractional crystallization of a crustal derived- primitive granitic melt to yield the differentiated monzogranites in the DIC; 3) the granodiorite shows abundant field and petrographic evidence for variable extent of mafic-felsic magma interactions (mingling, mixing and heterogeneous hybridization). Least squares mixing tests, using trace and major elements support the formation of the granodiorite rocks by a simple mixing of two end-members, the diorite and the less differentiated monzogranite. A proportion of the diorite end-member ranging between 15 and 50% can explain the observed chemical variations in the granodiorite.

Introduction

Felsic and mafic intrusive complexes and chemically equivalent volcanic rocks are abundant in the Proterozoic terrain of the Arabian-Nubian Shield. Understanding the origin of granitic rocks is a subject of longstanding interest, because it gives insight into the mechanisms that have operated during continental growth. The mafic intrusives mostly occur as large masses of metagabbro-diorite complexes which are interpreted by many workers as an integral part of an ophiolitic melange in the Egyptian basement complex (El Sharkawy and El Bayoumi, 1979; Hassanen, 1985). Recently, Mohamed and Hassanen (1996) and Takla *et al.* (1981), broadly subdivided the gabbroid rocks in Egypt into three major groups namely: ophiolitic metagabbro (O-type gabbro), arc-related, calc-alkaline metagabbro formed in a subduction environment (I-type gabbro) and the younger post-orogenic, unmetamorphosed arc gabbro (Y-type gabbro). Felsic intrusive rocks are often accompanied by extrusion of calc-alkaline, intermediate volcanic rocks (Stern and Hedge, 1985) locally contemporaneous with unmetamorphosed post-orogenic gabbros. This plutonic-volcanic complex is interpreted by El-Gaby *et al.* (1988) as cordillera-type association.

This paper presents new petrological, geochemical and isotopic data on the Dubr-Igla composite mafic-felsic intrusive complex (DIC) that crops out in the central eastern Desert (Fig. 1). These data are used to help constrain the origin

of the calc-alkaline granites in the Egyptian part of the Nubian Shield, their tectonic significance and the petrogenetic process(es) involved in the evolution of the continental crust in the Egyptian basement complex.

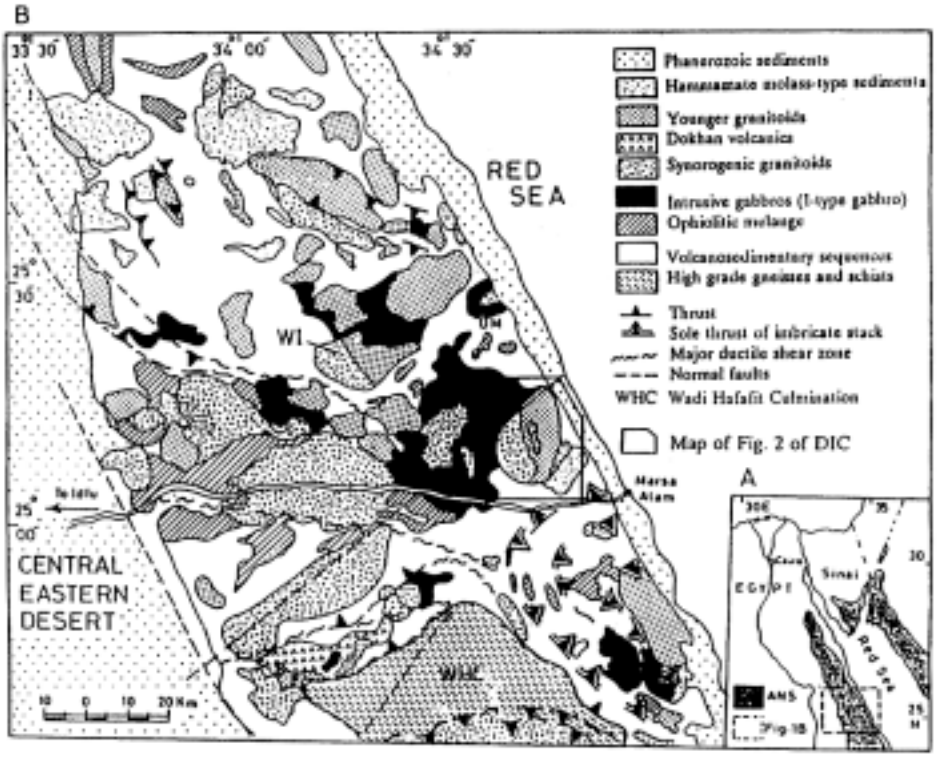

FIG. 1. Location of the Dubr-Igla intrusive complex (DIC) in relation to the major lithotectonic and structural elements in the central Eastern Desert of Egypt based on the geological map of Egypt 1:500,000 (Klitzsch *et al.,* 1987; Bennett & Mosley, 1987).

General Geology and Tectonic Setting

The Precambrian terrain in the central Eastern Desert (CED) consists of seven major lithological units (Fig. 1): 1) pelitic-psammatic schists and gneisses, 2) volcano-sedimentary sequences, 3) ophiolitic melanges, 4) synorogenic granitoids 5) calc-alkaline-intermediate volcanic rocks (Dokhan volcanics), 6) intrusive rocks ranging in composition from gabbro to granites (Younger granitoids) and 6) Hammamate molasse-type deposits (Akaad and El Ramly, 1960; Hassan and Hashad, 1990; El Gaby *et al.* 1988, 1990). The Dubr-Igla Complex (DIC) forms a suboval body exposed over about 240 km^2 at the extreme eastern border of the CED (Fig. 1). It is elongated in a NNW direction, parallel to the regional structural grains in the CED (Bennett and Mosley, 1987). The DIC rep-

resents an uplifted tectonic block, bounded by a broad brittle to ductile shear zone forming a dome-like structure (Stanek *et al.* 1993). Internal deformations within the rocks of the complex are minimal. The eastern and northern margins of the DIC are bordered by a belt (1-6 km wide) of acid volcanic rocks which represent the NE extension of the Um Khariga Formation (Akaad and Essawy, 1978). The acid volcanics, the upper part of Um Khariga Formation, consist of massive metapyroclastics and minor tuffaceous rhyolitic flows (Akaad and Essawy, 1978). These volcanics have major and trace element composition characteristic of calc-alkaline rocks with arc-affinity (Abu El-Ela, 1991). The Um Khariga acid volcanics are unconformably overlain by molasse-type sediments (Igla Formation; Akaad *et al.* 1977) which were deposited SE of the DIC (Fig. 2). The contacts with the latter are sharp and dip steeply under the Igla Formation with lack of any thermal effect. The Igla Formation consists of a sequence of interbedded conglomerates, greywackes and siltstones that were deposited in a NNE-SSW trending dextral strike-slip pull-apart basin (Rice *et al.* 1993).

The eastern and southern margins of the DIC are flanked by a thick sequence of volcanosedimentary rocks (Igla Eliswid Formation; Akaad *et al.* 1977). These rocks are highly deformed and foliated, generally parallel to the intrusive contacts of the DIC. The volcanosedimentary sequence shows complex and wide lithological variation. The metavolcanics include metabasalts, metadolerite, metadacite and meta-andesite. They are overlain by and interbedded with metasediments of biotite/chlorite schists, metagreywacke, phyllite and metasiltstone. Dyke swarms, having bimodal composition, cut across the DIC and its adjacent rocks. They include granite porphyry, aplite, diabases and basalts and minor andesite porphyry and comptonite. These dykes vary from 0.5 to 2 m in width and from few tenths of meters up to 2 km in length. The dykes follow two distinct trends, the most dominant trends NE-SW, related to the NW-SE transtension tectonic (*Stanek et al.* 1993). The latter gave way to late- to post-orogenic uplift of the deep-seated crustal block of the DIC (Stanek *et al.* op. cit.). The second set trends NW-SE are parallel to the elongation of DIC and to the Red Sea rift.

The Dubr-Igla Intrusive Complex (DIC)

Field observations and petrography

The DIC forms a suboval composite batholith 22 km long and as much as 16 km wide. The mafic and felsic intrusive suites in the DIC show a wide compositional variation from olivine gabbro and metagabbro to granite and granophyre. The mafic suite is represented by three rock types of different abundances in the mapped area. These are metagabbro, olivine gabbro (younger gabbro) and diorite-quartz diorit. The mafic suite forms an arcuate mass dominated by diorite

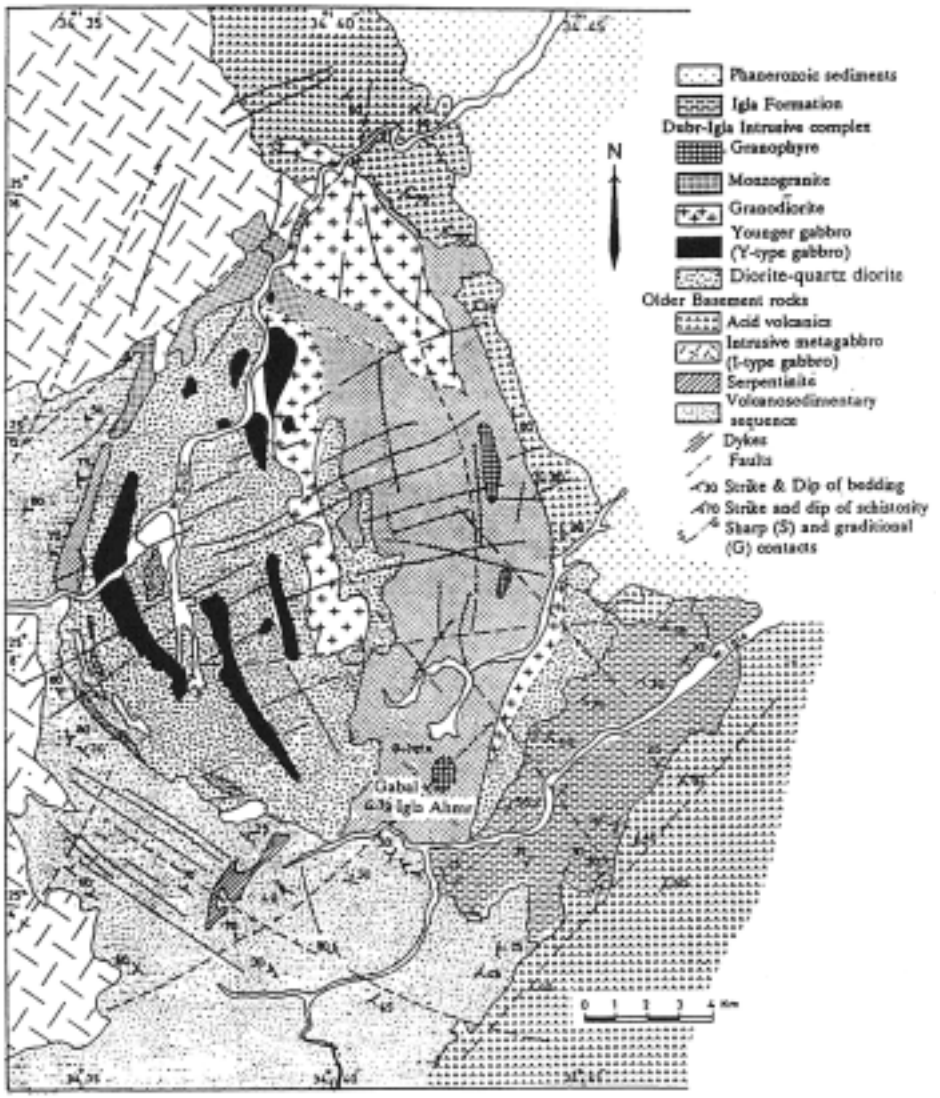

FIG. 2. Detailed geological map of the Dubr-Igla intrusive complex (DIC) and associated lithologies.

and quartz diorite chaotically interlayered with younger gabbro. Olivine gabbro and subordinate gabbronorite and hornblende gabbro occur in the diorite massif as nearly vertical sheets and minor irregular and lens-shaped outcrop patterns. The metagabbro occurs as a large massive body occupying the eastern and northeastern sectors of the mapped area (Fig. 2) and as small bodies of irregular shape scattered in the diorite-quartz diorite suite. The metagabbroic rocks are coarse grained, equigranular hypidiomorphic with blackish green color. They are metamorphosed up to epidote-amphibolite facies (Essawy, 1976). Relict igneous minerals include zoned plagioclase, clinopyroxene, magnetite and ilmenite, while chlorite, actinolite, epidote and quartz are common metamorphic products. Subophitic textures are common.

The diorite-quartz diorite occurs as two distinct masses. The largest mass occupies nearly the western part of the DIC outcrop with sharp and irregular contacts against the granodiorite-granite suite. The other mass is small and lies at the SE corner of the DIC (Fig. 2). The diorite-quartz diorites are massive to weakly foliated and medium- to coarse-grained but a fine-grained variety is also encountered. Contacts with the granodiorite show a gradational zone (up to 200 m wide) with extensive hybridization, particularly at the extreme SE part of the complex (Hassanen *et al.* 1996). In other places, sharp contacts and abundant mafic granular xenoliths are recognized where mingling has occurred (Fig. 3A). The rock consists of zoned plagioclase (An_{35} - An_{50}), green-brown to green hornblende, dark brown biotite and quartz. Accessory minerals include magnetite, ilmenite, titanite, apatite and scarce zircon.

The younger gabbro occurs in the diorite, mostly as sheets of about 10 m wide and extends discontinuously up to 3 km long. Small irregular and lens-shaped masses are also common. The olivine gabbro is the major component of the younger gabbro masses (Y-type gabbro; Fig. 2), while hornblende gabbro and gabbronorite are subordinate. The olivine gabbro is medium- to coarse-grained rocks, having textures characteristic of cumulates. The rocks consist of plagioclase (An_{75}-An_{85}; 40%-55%), clinopyroxene (30%-40%), olivine (5%-20%), hornblende (< 1%- 5%) and opaque minerals (5%-10%). Dark green to brownish green hornblende occurs as late-magmatic interstitial crystals and as post-magmatic patchy replacement of pyroxene. Accessory minerals include magnetite, ilmenite and apatite.

The monzogranites represent the second most abundant rock type, forming the whole eastern sector and the perimeter of the DIC. The monzogranites are nonfoliated, hypidiomorphic-granular rocks and subsolvous with pink to red color. The rocks consist of zoned plagioclase feldspar (An_{10} An_{20}), orthoclase perthite, quartz, hornblende and biotite. Apatite, zircon, allanite, titanite and minor opaque minerals are common accessories. The monzogranites are character-

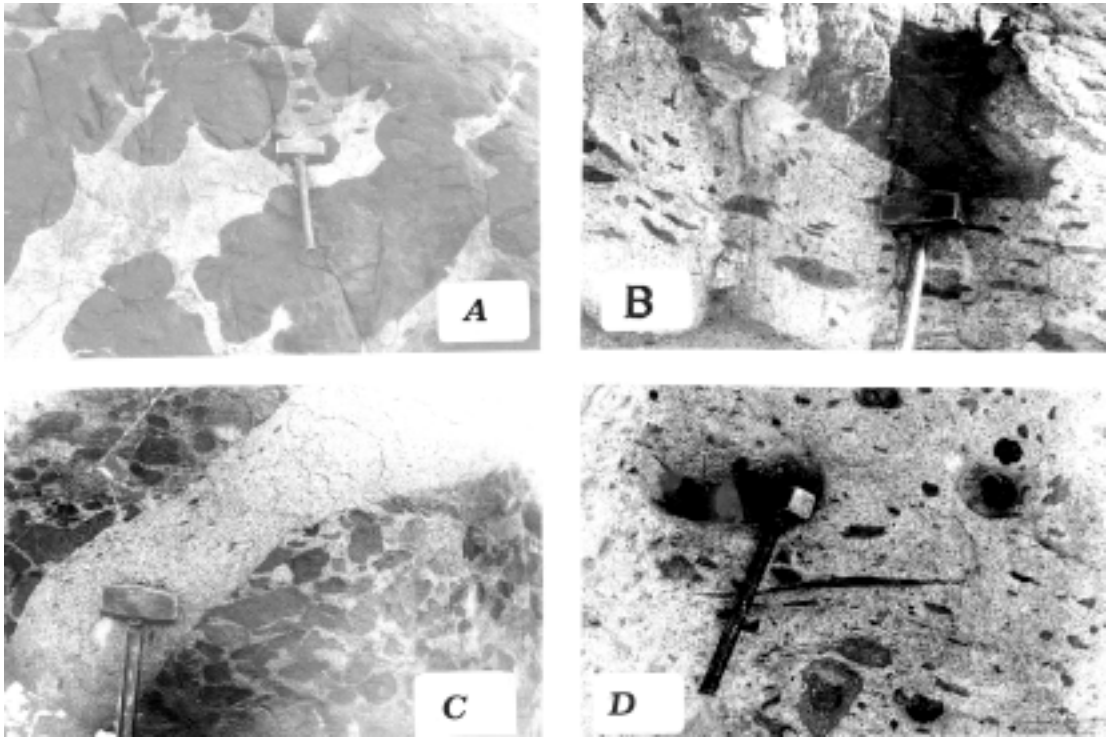

FIG. 3. Structural and contact relationships in the different intrusive phases in the Dubr-Igla complex. A – intermingling of quenched bulbs of meladiorite in host monzogranite showing characteristic cuspate and scaloped margins; B – flattened and parallel arranged mafic xenoliths in the granodiorite. C – granodiorite apophysis with very small and few xenoliths (represents homogeneous hybridization stage) remobilized and cut across, heterogenous hybridized granodiorite (early stage of mixing) with abundant, angular mafic xenoliths; D – xenoliths with different forms and size showing progressive stages of interaction with their host magma. These xenoliths are zoned with dark-coloured, mafic-rich core and relatively light-coloured outer-zone.

ized by the presence of few pegmatitic veinlets and miarolitic cavities and by the development of appinite at the granite diorite contact. Locally, the contact between the monzogranite and the diorite is gradational and diffused with development of hybrid zones of variable width (few centimeters up to tens of meters) having granodioritic composition. In other instances the contacts are sharp and display chilled and scalloped margins (Fig. 3A). This type of contact relationship is generally developed when mafic and felsic magmas are mixed in high-level plutonic settings (Taylor *et al.* 1980; Marshall and Sparks, 1984) and requires that the diorite should by liquid when it came in contact with the felsic magma.

The granodiorite is characterized by abundant mafic xenoliths, and their abundance and size decrease irregularly away from the mafic contact over a zone as wide as 300 m. Primary foliation in the granodiorite is defined by the flattened and parallel mafic xenoliths (Fig. 3B & D). The contacts of the granodiorite and monzogranite are also gradational and diffuse, which make contact delineation difficult to recognize and based approximately on the disappearance of the xenoliths in the rocks. The granodiorites are medium- to coarse-grained rocks with hypidiomorphic texture consisting of strongly zoned plagioclase (An_{27-52}), quartz, hornblende, biotite and minor K-feldspar. Apatite, zircon and ilmenite are accessory phases. The granodiorite near the contact with diorite shows irregular variation in mafic mineral content over a distance of a few centimeters to a few meters.

Microgranular mafic enclaves

Well-rounded ellipsoid microgranular mafic enclaves in the granodiorite are frequent and show different degrees of interaction with their host. They show marked variation in their abundance constituting more than 50% of the outcrop in a matrix of coarse-grained granodiorite imparting agmatitic-like structure (Fig. 3C). The enclaves have sharp, cuspate margins convex toward the host with fine-grained and hypidiomorphic granular to seriate texture. Some of them are zoned with gradation and diffused contacts (Fig. 3D) and show evidence of progressive stages of interaction with their host magma, similar to those reported from mixed-magma intrusions (Taylor *et al.* 1980; Hildreth, 1981). They display dark-colored, mafic-rich core of dioritic composition and an outer zone of relatively light colored diorite or mafic-rich granodiorite and grade outward into granodiorite matrix (Fig. 3D). Mineralogical composition of the enclaves is similar to their host granodiorite with plagioclase crystals (An_{40}-An_{50}) as the major abundant constituent (up to 60%), hornblende and biotite (30%-35%) and accessories (interstitial quartz, apatite, zircon, titanite, magnetite titanomagnetite and ilmenite). Apatite crystals in the enclaves are acicular (axial ratios as high as 40:1), smoky, pale brownish to greenish core and colorless rim.

Similar acicular apatite morphology has been produced experimentally on thermal quenching (Wyllie *et al.* 1962) and are present in some rapidly crystallized plutonic rocks (Reid *et al.* 1983)

Sampling and Analytical Techniques

On the basis of field observations and petrographic studies, forty-two samples from the different rock units in the DIC, mafic xenoliths and spatially associated metagabbro were carefully selected for geochemical analyses. Owing to the coarse to medium grain size of the rocks, large samples (average 4-5 kg in weight) were collected and reduced to powder before analyses. Twenty samples were analyzed at the Technical University of Berlin, Germany and the others at Bergen University, Norway. Major elements were determined by energy dispersive X-ray fluorescence (XRF) on fused pellets. Trace elements (except Hf) were also determined by XRF technique, but using pressed pellets and polyvinyl alcohol as the binding agent. Concentrations of rare earth elements (REE) and Hf were determined by an inductively coupled plasma source emission spectrometer (ICP-ESA) at the Special Research Project Arid Areas "SFB 69", TU, Berlin, Germany, according to the method of Walsh *et al.* (1981). Values for loss on ignition (LOI) represent the percentage of weight loss following repeated heating at 1000 C of a preweighed sample. The precision for major element analyses is within ± 5% for the amount present (± 2% for SiO_2); trace element precision range from 5% to 10%. Absolute accuracy of the REE has been assessed by comparison with international reference materials analyzed along with the samples and generally is better than 10%. Analytical results for representative samples are listed in Table 1 (Tables containing all analyses used in this work are available from the author upon request).

The Rb-Sr and Sm-Nd isotope analyses were performed at the Mineralogical-Geological Museum, University of Oslo (eight Samples) and in the Bergen University, Norway (eleven samples). The chemical separation procedures for Sr and Nd isotope analyses were those described by Pin and Carme (1987) and were determined by isotopic dilution. Total blanks are typically 1 ng for Nd and Sr and thus are negligible for this study. Isotope ratios were measured on a fully automated Five-Collector Vacuum Generators 354 (Oslo), and on ISOMASS VG 54E mass spectrometers (Bergen University). The decay constants used were $\lambda Sm = 6.54 \times 10^{-12\ y\text{-}1}$ and $\lambda Rb = 1.42 \times 10^{-11\ y\text{-}1}$ εt^{Nd} and εt_{Sr} values were calculated relative to CHUR with present day $^{147}Sm/^{144}Nd = 0.1967$, $^{143}Nd/^{144}Nd = 0.512636$, $^{87}Rb/^{86}Sr = 0.0736$ and $^{87}Sr/^{86}Sr = 0.70391$ (Allégre *et al.* 1983). The least square isochron lines and other isotopic parameters were computed using the computer program "Isoplot" by Ludwig (1991) and the results are presented in Table 2.

TABLE 1. Representative major and trace element contents in the granitoid rocks and xenoliths in the Dubr-Igla intrusive complex, Egypt.

Rock type	Metagabbro			Gabbro			Diorite-quartz diorite		
sample N	675	683	685	630	635	636	966	968	972
SiO_2	49.90	52.16	50.11	48.14	50.83	49.63	56.62	56.35	61.28
TiO_2	1.13	1.55	1.45	1.08	1.12	1.01	0.68	0.61	0.57
Al_2O_3	16.41	16.76	16.31	17.26	16.06	17.12	17.10	16.23	15.62
Fe_2O_3	9.94	8.99	8.76	9.41	9.09	9.50	7.40	7.05	5.70
MnO	Bd	Bd	Bd	Bd	Bd	Bd	0.12	0.13	0.12
MgO #	8.43	6.64	8.73	10.61	9.65	9.14	5.41	5.18	3.49
CaO	9.75	8.55	9.31	10.31	8.71	11.33	7.14	7.09	5.29
Na_2O	2.57	2.88	2.61	2.23	2.52	2.26	2.57	2.47	2.67
K_2O	0.51	0.60	0.55	0.13	0.48	0.17	1.41	1.74	2.30
P_2O_5	0.08	0.19	0.13	0.06	0.10	0.06	0.19	0.15	0.
LOI	0.81	0.92	0.87	0.89	0.81	0.59	1.32	2.16	2.35
Total	99.53	99.24	98.83	100.1	99.37	100.8	99.96	99.16	99.53
Mg No.	62.68	59.39	64.34	67.77	69.07	65.58	59.15	59.27	54.80
Trace elements (ppm)									
Cr	158	506	232	649	851	339	103	131	81
Ni	71	437	88	1525	1056	59	55	57	35
Co	70	34	45	42	34	73	20	31	49
Sc	266	34	31	32	32	43	22	27	15
V	215	246	219	211	196	239	237	207	155
Rb	8	14	11	6	8	12	27	36	28
Ba	100	76	82	39	101	53	406	542	774
Sr	252	174	182	188	173	193	463	445	388
Ga	19	15	16	11	13	15	15	14	16
Nb	3	1	2	Bd	1	Bd	3	2	3
Zr	75	65	70	61	87	55	55	63	92
Y	31	30	27	22	26	21	16	16	21

Rock type	Xenoliths			Granodiorite			Monzogranite		
sample N	655*	653**	651	661	666	680	646	667	506
SiO_2	69.32	68.95	70.67	71.43	70.84	73.71	75.92	75.52	73.89
TiO_2	0.36	0.38	0.34	0.33	0.27	0.25	0.19	0.19	0.20
Al_2O_3	14.71	14.83	15.10	14.86	14.47	13.31	13.01	13.07	13.34
Fe_2O_3	3.11	3.62	2.90	2.65	2.19	2.26	1.70	1.80	2.28
MnO	Bd	Bd	Bd	Bd	Bd	Bd	Bd	Bd	Bd
MgO #	0.76	0.82	0.56	0.69	0.56	0.54	0.23	0.23	0.14
CaO	2.35	2.63	2.39	2.30	2.11	1.40	0.92	0.94	0.63
Na_2O	3.11	3.21	3.88	3.71	3.69	3.70	3.52	3.54	3.45
K_2O	3.61	2.85	2.39	2.73	3.01	3.31	3.48	3.54	3.89
P_2O_5	0.06	0.07	0.06	0.06	0.04	0.04	0.03	0.03	0.08
LOI	1.65	1.72	0.88	1.69	1.59	1.32	1.10	0.89	1.22
Total	99.04	99.08	99.17	100.5	98.77	99.84	100.1	99.75	99.12
Mg No.	32.61	30.97	27.66	34.02	33.62	32.12	21.13	20.19	10.84
Trace elements (ppm)									
Cr	12	17	18	15	13	23	7	14	15
Ni	25	29	34	23	34	31	12	18	2
Co	15	14	Bd	Bd	11	13	15	18	Bd
Sc	13	12	10	14	Bd	Bd	Bd	5	8
V	39	38	34	28	26	21	17	19	8
Rb	57	55	50	62	68	69	78	71	82
Ba	455	460	453	417	444	414	452	438	395
Sr	166	177	144	126	111	95	64	62	60
Ga	14	16	11	13	19	19	18	18	16
Nb	8	6	4	6	7	6	7	7	12
Zr	170	163	236	215	188	170	172	176	155
Y	34	32	30	40	38	38	44	40	33

TABLE 1. (Continued)

Rock type	Metagabbro			Gabbro			Diorite-quartz diorite		
sample N	675	683	685	630	635	636	966	968	972
Th	6	8	6	Bd	5	4	4	6	6
U	Bd	Bd	Bd	Bd	Bd	Bd	Bd	4	2
F	nd	nd	nd	nd	nd	nd	nd	nd	nd
Hf	2.3	2.4	1.3	1.7		6.9	4.8	5.2	
La	7.1	4.3	5.2	1.8		2.6	8.9	5.7	
Ce	20.0	12.3	15.3	7.3		8.4	22.4	15.3	
Pr	nd	1.4	2.4	1.3		1.5	Bd	Bd	
Nd	13.1	8.2	9.8	5.7		7.6	11.7	9.4	
Sm	4.2	3.5	3.8	2.1		3.0	3.2	2.4	
Eu	1.6	1.3	1.4	1.0		1.4	0.9	0.8	
Gd	4.6	4.0	3.3	2.9		3.7	3.2	2.5	
Dy	5.1	5.2	4.3	3.5		3.9	0.0	0.00	
Ho	1.1	1.0	0.9	0.6		0.8	0.7	0.5	
Er	2.9	2.8	2.1	2.3		2.7	Bd	Bd	
Yb	3.1	3.0	2.6	2.2		2.7	1.6	1.1	
Lu	0.4	0.4	0.3	0.3		0.5	0.3	0.2	

Rock type	Xenoliths		Granodiorite				Monzogranite		
sample N	655*	653**	651	661	666	680	646	667	506
Th	11	9	14	16	17	19	18	19	17
U	5	4	5	6	5	6	5	6	3
F	nd	nd	733	630	630	1053	nd	467	nd
Hf			6.8	4.9	6.6	6.9	6.9	8.7	6.5
La			16.0	18.0	17.2	22.0	30.0	75.0	28.0
Ce			28.0	41.0	32.0	49.0	64.0	158	62.0
Pr			3.3	5.0	4.0	4.7	7.6	17.0	6.6
Nd			16.0	25.0	20.0	20.0	27.0	81.0	25.0
Sm			4.4	6.5	5.3	4.8	6.5	13.0	5.9
Eu			1.0	1.2	1.1	0.7	0.6	1.2	0.7
Gd			3.9	5.6	Bd	4.6	5.7	9.9	5.6
Dy			4.5	6.3	Bd	5.9	7.4	9.9	6.5
Ho			1.1	1.2	1.2	1.2	1.5	1.9	1.3
Er			3.0	4.0	3.6	4.1	4.8	6.5	4.0
Yb			3.5	4.6	4.2	4.9	5.7	7.2	4.8
Lu			0.6	0.7	0.6	0.7	0.8	1.1	0.7

*Total iron as Fe_2O_3 **Xenoliths in granodio nd = not determined
#Mg no. = (Mg/Mg + Fe) × 10 Bd = Below detection limit

TABLE 2. Rb-Sr and Sm-Nd isotope data and parameters of the different rocks units in the Dubr-Igla complex and crustal rocks from the Eastern Desert, Egypt.

Sample no.	Rb (ppm)	Sr (ppm)	$^{87}Rb/^{86}Sr$	$^{87}Sr/^{86}Sr^{a}$ +/−2	$^{87}Sr/^{86}Sr^{c}$ (initial)	Sr	Sm (ppm)	Nd (ppm)	147Sm/144Nd	143Nd/144Nd +/−2	(143Nd/144Nd) (initial)	Nd	$T^{\#}_{DM}$
Monzogranites 644 +/− 7 Ma													
663	98.2	81	3.522	0.735006 +/−26	0.703343	−16.42	15.1	65.8	0.1457	0.512580 +/−33	0.511990	3.83	0.86
667	105.8	65	4.721	0.746335 +/−28	0.703107	−19.76	22.9	79.3	0.1765	0.512747 +/−24	0.521005	3.67	0.98
660	107.6	103	2.993	0.730611 +/−14	0.70291	−22.56	17.5	32.8	0.3267	0.513391 +/−15	0.521020	3.96	0.53
646	67.1	66	2.885	0.729409 +/−16	0.702453	−29.04	16.4	26.5	0.3801	0.513671 +/−11	0.512080	5.15	0.62
680	30.2	97	0.882	0.711112 +/−12	0.702872	−23.10	13.8	30.1	0.2835	0.53257 +/−27	0.512070	5.11	0.59
707	132.3	95	4.025	0.739840 +/−18	0.702878	−23.01	11.5	68.6	0.1029	0.512475 +/−24	0.512044	4.44	0.72
709	60.9	70	2.553	0.726482 +/− 2	0.703421	−15.30							
702	112.7	78	4.208	0.741896 +/−16	0.70354	−13.62							
Granodiorites 614 Ma													
666	126.2	105	3.704	0.735514 +/−18	0.703076	− 9.95	3.3	21.4	0.0924	0.512423 +/−14	0.512051	3.82	0.73
661	108.1	120	3.629	0.725606 +/−20	0.702578	−17.02	6.1	24.7	0.1511	0.512697 +/−21	0.512089	4.55	0.74
643	103.8	112	2.667	0.726101 +/−18	0.702739	−14.73	9.6	16.7	0.3515	0.513491 +/−12	0.512077	4.31	0.54
Diorite-quartz diorites 704 +/− 13 Ma													
996	22.3	475	0.159	0.703881 +/−11	0.702233	−28.04	2.7	11.3	0.1454	0.512780 +/−12	0.512101	7.06	0.52
968 - B	32.4	326	0.286	0.705122 +/−13	0.702234	−32.15							
971	26.5	371	0.205	0.704351 +/−13	0.702286	−31.42	2.1	9.8	0.1316	0.512684 +/−16	0.512082	6.68	0.59
517	60.5	284	0.615	0.708451 +/−02	0.702289	−31.37	2.9	13.4	0.1307	0.512781 +/− 5	0.512173	8.46	0.43
968	19.7	577	0.096	0.703221 +/−28	0.702248	−31.95	2.4	9.2	0.1625	0.512823 +/− 6	0.512090	6.84	0.52
Younger Gabbro 573 Ma$													
630	6.4	290	0.073	0.703020 +/−12	0.7026	−16.50	1.2	4.6	0.1470	0.512727 +/− 2	0.512024	4.83	0.76
Metagabrro 881 +/− 58 Ma													
675*	17.6	549	0.092	0.703531 +/−10	0.702374	−15.44	3.6	13.5	0.1596	0.512902 +/− 7	0.512782	9.17	0.324
685*	12.2	463	0.081	0.703498 +/−35	0.702483	−13.89	2.4	11.4	0.1275	0.512639 +/− 6	0.511903	7.64	0.645
Crustal rocks													
A-LC *1	1.72	614	0.021	0.40333	–	–	2.8	10.3	0.1810	0.51280	–	5.23	–
86AZ47B *2	25.85	116.9	0.64	0.712030 +/−30	0.707104	46	2.15	7.89	0.0160	0.51274 +/−20	0.512174	4.35	–

a & b Uncertainties are two standard deviations of the mean; c = Calculated initial ratios, using ages and uncertainties in Fig. 7.

≠ Depleted-mantle model ages in Ma (TDM) using present-day values of (143Nd/144Nd) DM = 0.513151 and (147Sm/143Nd) DM = 0.21357.

*1 Mean of mafic metaigneous xenoliths (lower crust) from Saudi Arabia (McGuire and Stern 1993).

*2 Felsic granulite xenolith (lower crust) from Zabargad Island, Red Sea (Lancelot and Bosch, 1991).

* Metagabbro; $ = Olivine gabbro calculated parameters using assumed age 573 Ma.

Geochemistry of the Dubr-Igla Complex

Rock classification and compositional variation

The plutonic rocks in the Dubr-Igla complex display a wide range of compositional variation from gabbroic to granitic compositions (SiO_2 = 48-75%, MgO = 0.6-10 % and K_2O=0.13-5.5 %). The present sampling does not reveal any spatial zoning, although granophyre is typically more abundant at the top of the plutons (Hassanen *et al.* 1996). The DIC intrusive rocks and the metagabbro have calc-alkaline affinity (or subalkaline: Irvine and Baragar, 1971)(Figs. 4A and B). The DIC rocks plot in the calc-alkaline field of Ringwood (1975); while the granitic samples cluster as a distinct group near the alkali apex (Fig. 4C). The chemical variations , in terms of Harker diagrams, of the different DIC rock units are summarized in Fig. 5. In these diagrams, the basic through intermediate to acidic rocks are all distributed along more or less regular trends (Al_2O_3, MgO, P_2O_5, Sr, V, Ni, CaO, Fe_2O_3 and K_2O) with a compositional gap between 61% -67% SiO_2. With increasing SiO_2, the elements Rb, K and Ba increase, while Ca, P, Ti, Al, Fe, Sr and Ni decrease. These major and trace element variations are similar to other mafic-felsic intrusive rocks from the eastern Desert of Egypt (*e.g.* Wadi El-Imra district, El-Sayed, 1994; Furnes *et al*. 1996) and from the Arabian Shield (Jackson, 1986). The olivine gabbro samples are characterized by wide range of abundance of Ni (31-521 ppm), high Cr and V (153-851 ppm and 196-246 ppm, respectively) and low content in Rb, La, Nb, Y and Zr (Table 1). They have a transitional tholeiitic to calc-alkaline affinity (Figs. 4 B&C), very low K_2O/Na_2O (< 0.1), high Al_2O_3 (16.84-18.48) and wide range of Mg-number (Mg/Fe+Mg =53.6-69.1). In spite of the compositional overlap between the olivine gabbro and the metagabbro, the latter has lower MgO, Ni, Cr and Zr/Y ratio and higher P_2O_5, K_2O, REE, La/Yb_n and K_2O/Na_2O than the olivine gabbro. In terms of major and trace elements, both the olivine gabbro and metagabbro more closely resemble island arc basalts related to subduction (White and Patchett, 1984).

The granitic rocks in the DIC (monzogranites) have 70-75% SiO_2, a moderate range in K_2O/Na_2O (0.89-1.21) and lower levels of compatible elements (Ni, Cr, V, Sc, Sr, Y) and higher contents of Rb, Nb and Zr than that of the diorite and quartz diorite (Table 1). The rocks are mildly peraluminous (CNK= 0.95 - 1.18) with 0.8% to 3% normative corundum. The average (10^4Ga) /Al ratio is 1.99 in the DIC monzogranites and thus very close to that of the typical M-type (1.87) and I-type granites (2.1) as defined by Whalen *et al.* (1987). These rocks belong to the post-orogenic granite group according to the classification of Rogers and Greenberg (1990) with arc affinity (Figs. 6 A and B).

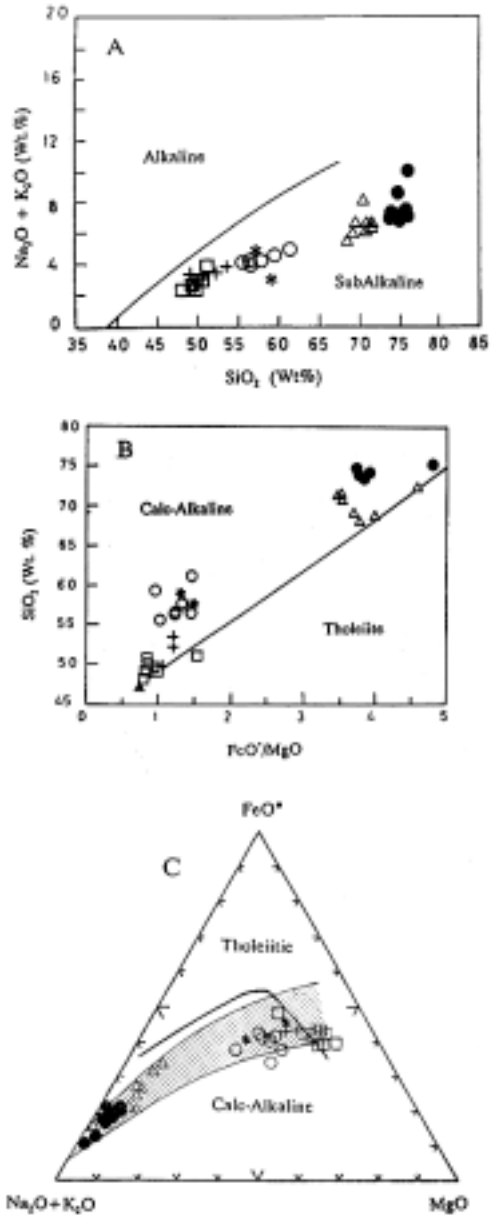

FIG. 4. Compositional variation of the intrusive phases in the ($Na_2O + K_2O$) – Si O_2 (A), FeO/MgO – SiO_2 (B) and in the FeO – ($Na_2O + K_2O$) – MgO (C). Rock symbols : ●, monzogranite; Δ, granodiorite; ○, diorite-quartz diorite; ⁎, xenolith in granodiorite; + , metagabbro (I- type); □, olivine gabbro (Y-type). Stippled area in (C) represents the orogenic calc-alkaline field (after Ringwood, 1975).

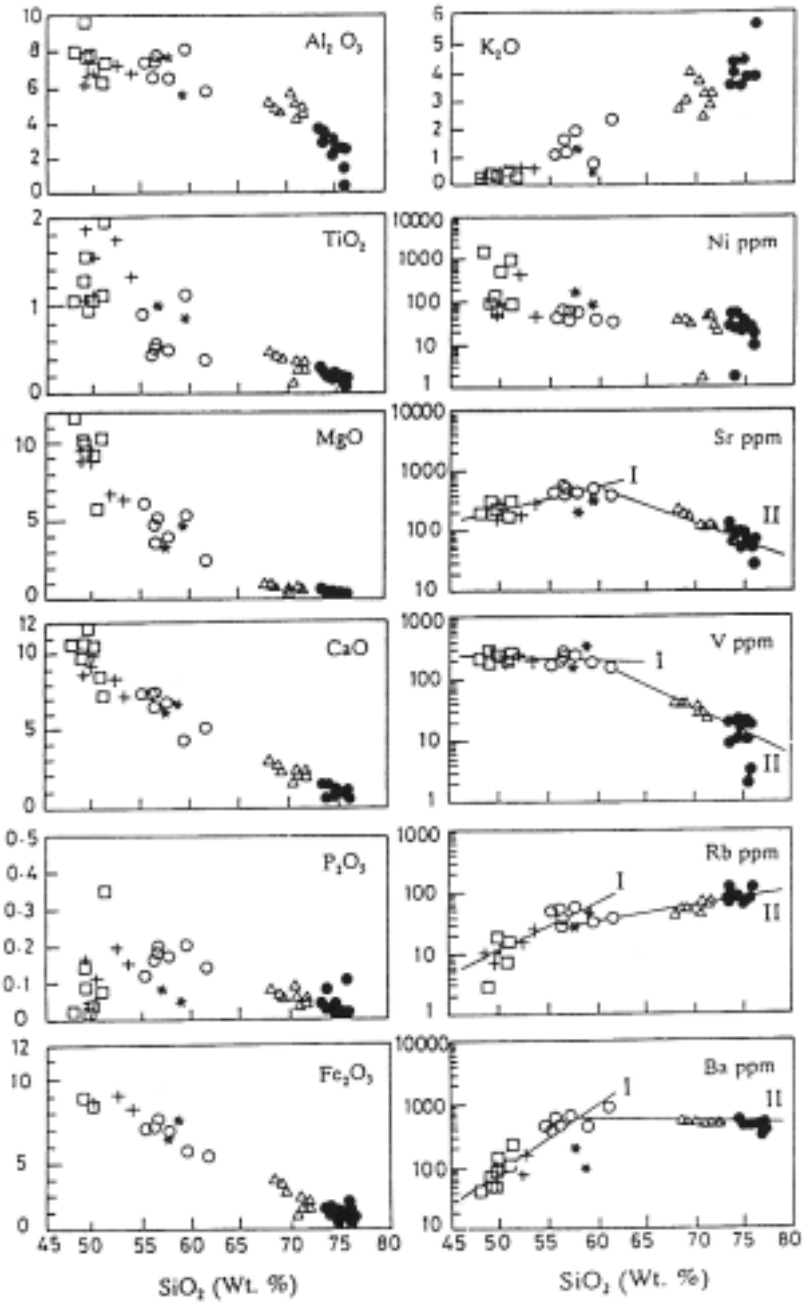

FIG. 5. Harker variation diagrams for selected major and trace elements in the DIC. Lines I & II represent the general trends of the mafic-intermediate and felsic suites respectively. Symbols are as in Fig. 4.

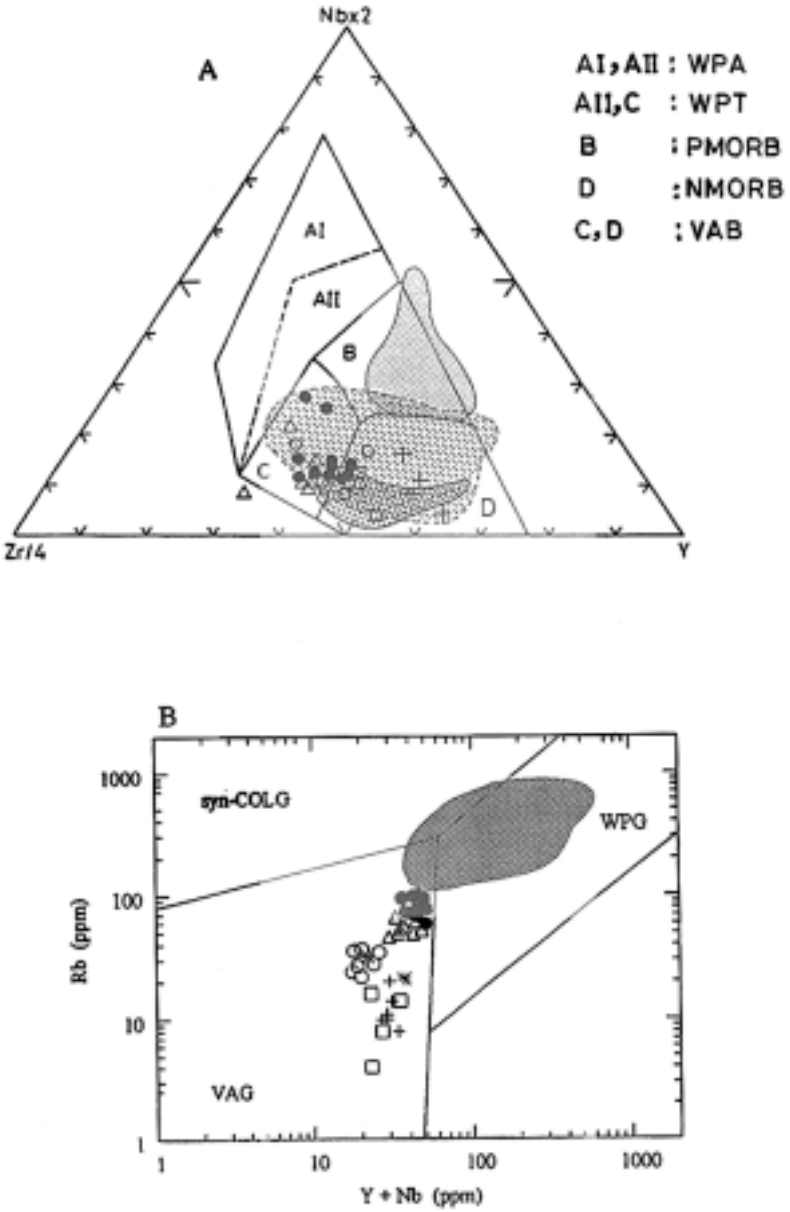

FIG. 6. The rocks of the DIC plotted in (A) Nb*2 - Zr/4- Y (Mescheda 1986) and (B) Rb (Y + Nb) (Pearce *et al.,* 1984). Fields in (A) from Mohamed and Hassanen (1996) and represent Y-type gabbro (heavy stippled area), I-type gabbro (dashed area) and O-type gabbro (light stippled area). Field in (B) includes Egyptian post-collision, A-type granites based on data from Hassanen & Harraz (1996), Hassanen *et al.* (1995). WPG = within-plate granites; VAG = volcanic arc granites; syn-COLG = syn-collision granites; WPA = within-plate alkali basalts; WPT = within-plate tholeiites; MORB = mid-ocean ridge basalts; VAB = volcanic arc basalts.

Compatible/incompatible element relationship

Several covariation plots involving major and trace elements were tested to determine possible petrogenetic processes and source region(s) that control the composition and evolution of the rock units of the DIC. Two such examples are presented in Figs. 7A and B, which reveal two distinct trends: 1) a negative correlation of CaO and Sr and Ba; 2) positive correlation between CaO and Sr and Ba. Similar behavior and trends are also recognized on the companion diagram of V versus Rb (Fig. 8). The Rb/Sr versus 1/Sr plot (Fig. 9) displays a straight-line trend for the diorite-granodiorite-granite association indicative of mixing processes (Langmuir *et al.* 1978). The mafic rocks fall out of this trend and therefore cannot be an end-member for this association.

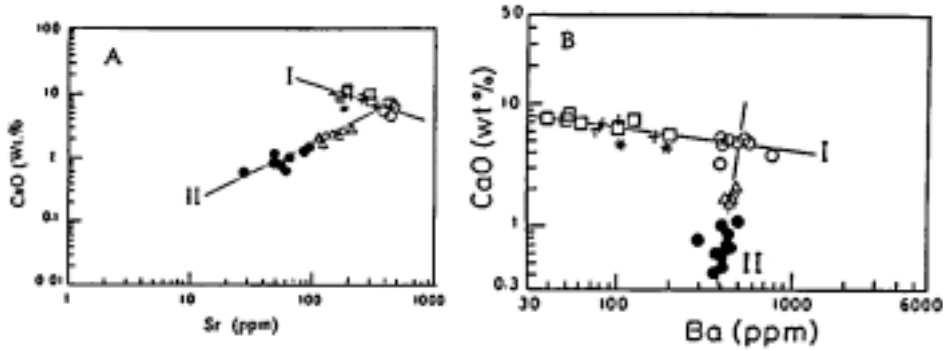

FIG. 7. The binary variation diagrams of CaO (wt. %) versus Sr (ppm) and CaO (wt. %) versus Ba (ppm) (B) for the different intrusive phases in the DIC. The trends I & II and symbols are as in Fig. 4.

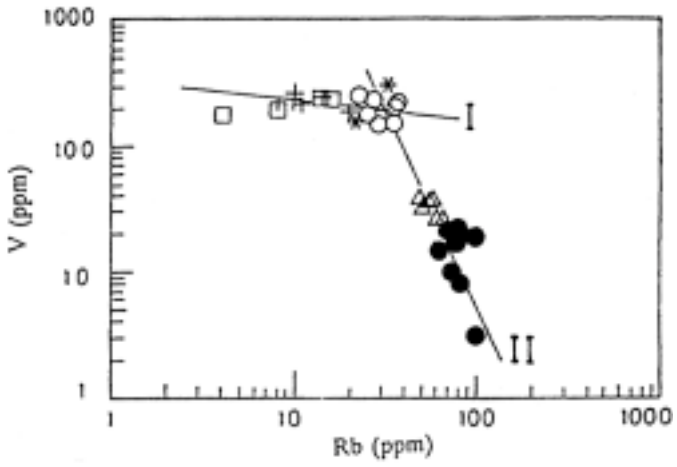

FIG. 8. Plot of V (ppm) vs. Rb (ppm). Trends I & II as in Fig. 5. Symbols are the same in Fig. 4.

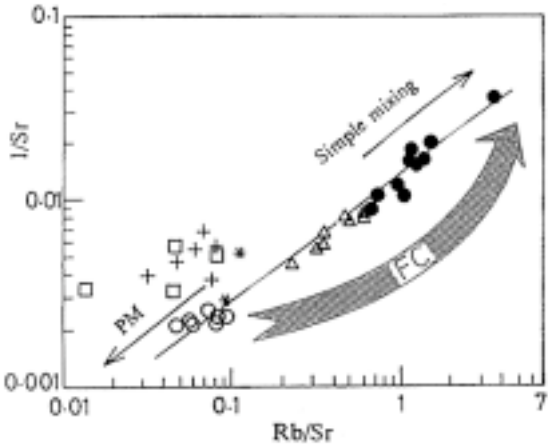

FIG. 9. Diagram Rb/Sr - 1/Sr. The heavy stippled arrow (FC) indicates a general trend of fractional crystallization. PM is the partial melting trend. Symbols as in Fig. 4.

Rare earth element geochemistry

REE analyses of representative samples from the DIC are summarized in Table 1, and presented in Fig. 10. The intrusive rocks show an increase in the total REE (31-381 ppm) and weakly fractionated REE patterns (La/Yb_n = 0.96-6.97) with increasing SiO_2 content. The metagabbros show a nearly uniform flat and depleted REE pattern (La/Yb_n =0.96-1.53) with weak positive Eu anomalies (Eu/Eu^* = 1.06-1.21) similar to those of immature island-arc tholeiites (White and Patchett, 1984) or intra-oceanic back-arc basin volcanics (Saunders and Tarney, 1979). The olivine gabbro is characterized by low REE content and depleted LREE (La/Sm_n = 0.5-0.53) with moderate positive Eu anomalies (Eu/Eu^* = 1.24-1.28) combined with the high Ni and Cr content. This confirms the cumulate nature of this rock.

Two analyses of the diorite rocks display fractionated REE pattern (La/Yb_n = 3.72-3.47) and barely detectable or indistinct Eu anomalies. The granodiorites and monzogranites have the same overall REE pattern shape (Fig. 10) and flat patterns in the HREE region (Gd/Yb_n = 0.93 and 0.89 on average respectively). The monzogranites have higher abundances of the total REEs, fractionated LREE (La/Sm_n = 2.83-3.56) and larger negative Eu anomalies (Eu/Eu^* = 0.46 - 0.30) than the granodiorites (Fig. 10). The monzogranites patterns are similar to the calc-alkaline magmatism from subduction zone environments (Martin, 1986). The development of negative Eu anomalies and concomitant Sr depletion in the DIC granitoids indicate that plagioclase is a major fractionated mineral.

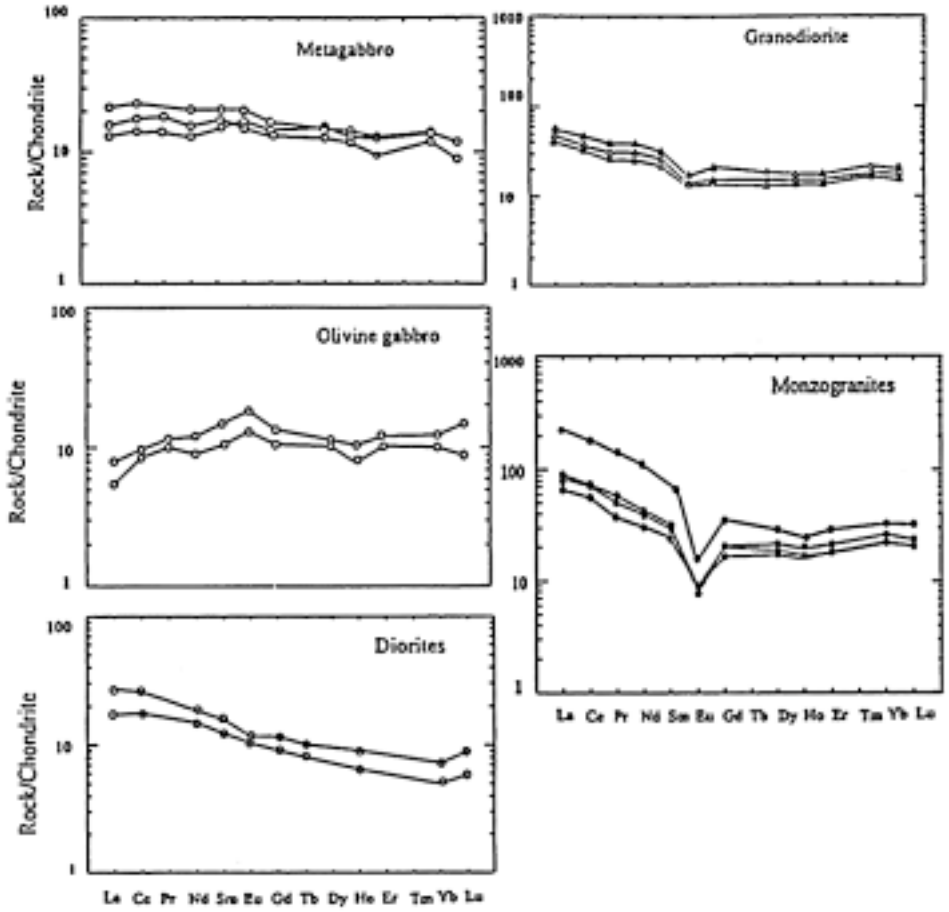

FIG. 10. DIC Chondrite-normalized REE patterns. Normalizing values from Sun (1982).

Sr and Nd Isotopic Data

Isotopic data of the different rock units from the DIC are shown in Table 2. Rb-Sr whole-rock regression line (Fig. 11B) for the monzogranite provides an age of 644 ± 7 Ma with an initial $^{87}Sr/^{86}Sr$ ratio of 0.7031 ± 0.0002. This age is interpreted as the time of emplacement of the calc-alkaline felsic intrusive suite of the DIC and fall within the range (675-500 Ma) of the second episode of igneous intrusion in the eastern Desert of Egypt (Hashad, 1980). Also, it is in agreement with 621 Ma for Gabal Igla Ahmr pluton (Hashad *et al.* 1972) and is similar to the age at 650 Ma for the late-tectonic calc-alkaline granites from Wadi El-Imra district (WI, 30 kms NW of the DIC, Fig. 1) (Furnes *et al.* 1996).

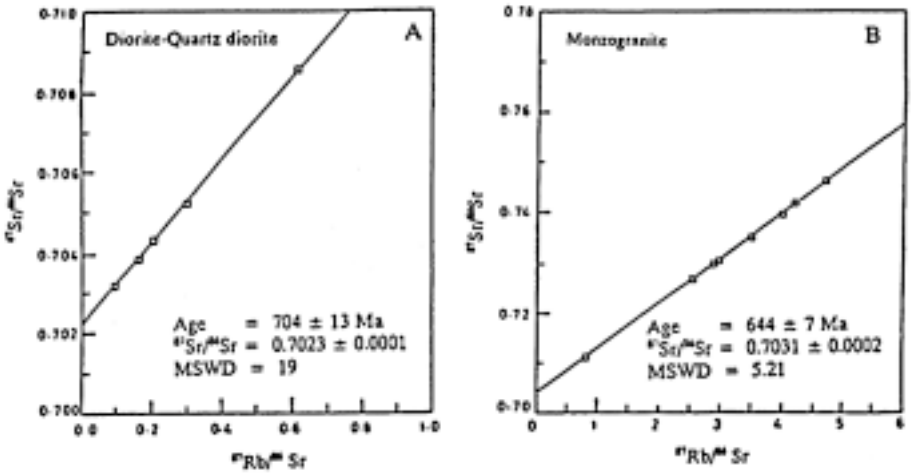

FIG. 11. Rb-Sr whole-rock isochron diagrams for the monzogranite (A) and diorite-quartz diorite (B).

The five analyzed diorite-quartz diorite samples yield an age of 704 ± 13 Ma (MSWD = 19), and an initial $^{87}Sr/^{86}Sr$ ratio of 0.7023 ± 0.0001 (Fig. 11A). A similar age of 709 Ma (single zircon model age, Stern and Hedge, 1985) was reported for tonalite (quartz diorite) from Wadi Kreiga. Also, U-Pb age on zircon from quartz diorite (Gabal Dahanieb, southeastern Desert) gave 711 Ma ± 7 Ma (Dixon, 1981). Gillespie and Dixon (1983) define a group of an older tonalite to granodiorite (OTG) suite, using Pb isotope data, with ages in the range 610-710 Ma. In spite of the high MSWD of the studied diorite- quartz diorite, the low intercept and comparison with other petrologically and chemically similar dated rocks in the Eastern Desert of Egypt indicate this age is probably close to the true age.

The intrusive ages of the other rock units in the DIC are still uncertain. Many workers reported the ages of granodiorites from different localities in the Eastern Desert. Kamel *et al.* (1983) dated a cycled gabbro-granodiorite form Umm Rus (UM, Fig.1) at 573-615 Ma. Also, granodiorite from Umm Gidri was dated at 593-615 Ma (K/Ar method, Kamel and Abel Aal, 1987). Stern and Hedge (1985) reported ages 614-620 Ma for granodiorites from different localities (Abu Ziran, Wadi Dib, and Wadi Hawashia) in the ED of Egypt. Accordingly, the initial Sr isotope, ϵ^t_{Nd} and ϵ^t_{Sr}, listed in Table 2, were calculated assuming ages of 614 Ma for the granodiorite, 880 Ma for the metagabbro (Abdel Rahman and Doig, 1987) and 573 Ma for the younger gabbro (Kamel *et al.* 1983). The low initial Sr ratios of the DIC (Fig. 13 and Table 2) fall within the range (0.702-0.704) reported by Stern and Hedge (1985) for all igneous rocks in the eastern Desert of Egypt.

The DIC Nd and Sr isotopic variation is reported in the ϵ^t_{Nd} - ϵ^t_{Sr} diagram (Fig. 12), in addition to the compositional fields of SE Sinai granites (Moghazi, 1994), wadi El-Imra granites, eastern Desert (Furnes *et al.* 1996), and the Arabian-Nubian Shield (ANS) basement rocks (Duyverman *et al.* 1982). In Fig. 12, the DIC granitoid and mafic rocks show a narrow range of initial Sr isotope ratios (0.7022-0.7035) and relatively more varied ϵ^t_{Nd} values (3.38- 9.15). All the DIC samples are clustered within the field delineated for the ANS and overlap those from the Egyptian basement complex. The wholly negative ϵ^t_{Sr} and positive ϵ^t_{Nd} values indicate a source region with high Sm/Nd ratio and suggest that the DIC protolith was either the mantle and/or juvenile crustal material derived from the mantle. Similar results are also reported for the mafic and granitoid rocks from Eastern Desert, Egypt (Furnes *et al.* 1996). Moreover, the DIC rocks show an inverse correlation between ϵ^t_{Nd} and ϵ^t_{Sr} (Fig. 12), which is probably a result of mixing or high-level assimilation-fractionation processes (AFC). However, the hypothesis of simple differentiation processes occurring within a chemically homogeneous reservoir is ruled out by the significant variability of Sm/Nd ratio (0.1-0.63) in the Dubr-Igla granitoids, since these processes do not greatly affect the Sm/Nd ratio (Allegre and BenOthman, 1980). The gabbroic and dioritic rocks show a restricted range of ϵ^t_{Nd} (6.68-9.15) and initial $^{87}Sr/^{86}Sr$ ratios (0.7022-0.7025) suggesting derivation from more depleted source such as the depleted mantle.

Discussion

The aims of this section are to constrain source region(s) of the DIC mafic-intermediate and felsic suites and the petrogenetic processes governing their evolution. This will help understand the processes that operated during growth of the Nubian Shield. The geochemical and isotopic data indicate that the mafic-intermediate and felsic suites cannot be derived from the same homogeneous source. In addition, no simple petrogenetic process can explain the whole chemical and isotopic variation in the different rock units of the DIC.

Source regions of the magma

In many orogenic, composite calc-alkaline granitoid plutons, the mafic suite may represent mantle-derived magmas (Whitney, 1988; Gasquet *et al.* 1992; Tepper *et al.* 1993; Dias and Leterrier, 1994). The composition of these magmas may be modified by crustal contamination, mixing with crustal-derived components or subduction processes (Ben Othman *et al.* 1984). The chemical composition of the mafic-intermediate rocks in the DIC is characterized by high Mg/Fe+Mg (62.9), Cr and Ni (300 ppm and 130 ppm), low Rb/Sr (< 0.1) and isotopic signatures of ϵ^t_{Nd} = 9.2 to 6.7 and ϵ^t_{Sr} 13.9 to -32.2. These features em-

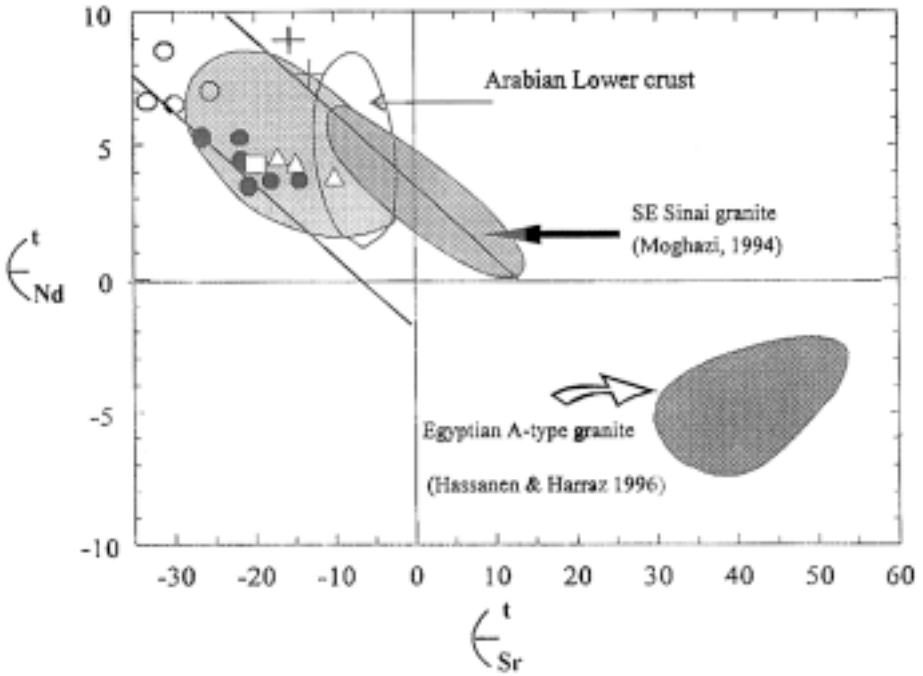

FIG. 12. ϵ^t_{Nd} vs. ϵ^t_{Sr} diagram for the DIC granitoids. Moderate and heavy stippled fields represent calc-alkaline granites from SE Sinai (Moghazi, 1994) and Egyptian A-type granites (Hassanen & Harraz, 1996) respectively. Light stippled area is the field of intrusives and extrusives from Arabian-Nubian Shield (Duyvermann *et al.* 1982; Stern & Kröner, 1993). Clear fields represents the Arabian-Nubian lower crust based on data from McGuire and Stern (1993) and the mantle array (O'Nions *et al.* 1979). Other symbols as in Fig. 4.

phasize that it has been derived from the mantle source without any significant crustal contamination. Therefore, the mafic-intermediate suite represents ultimate products from a depleted-type mantle-derived magma present in young orogenic area as primitive island arcs. Similar mantle source are also reported for some gabbro-diorite suites from the eastern Desert of Egypt (Dixon, 1981; Abdel Rahman, 1990; Furnes *et al.* 1996).

The isotopic composition of the felsic suite (monzogranite) is characterized by ϵ^t_{Nd} = 5.2-3.4 and $^{87}Sr/^{86}Sri$ = 0.7024-0.7035 which is incompatible with derivation from an old upper crustal source. From an isotopic point of view, it is impossible to distinguish between juvenile lower- crustal material or direct partial melting of the mantle. However, the second alternative can be rejected if we consider the trace element data and experimental work (Rapp and Watson, 1995). Experimental works show that melting of underplated mafic lower crust could produce felsic magmas with I-type composition (Rushmer, 1991; Wolf and Wyllie, 1994; Rapp and Watson, 1995). Studies on granulite xenoliths from

the lower crust (Mittlefehldt, 1983; Lancelot and Bosch, 1991; McGuire and Stern, 1993) indicate that the Arabian continental lower crust is dominated by mafic, meta-igneous granulites. The above discussion suggests that the DIC protolith was depleted mantle and juvenile crustal material (sub-arc crust) that had been separated from the mantle.

Petrogenesis of the mafic-intermediate suite

The Sr-Nd isotopic data of the metagabbro, their low Rb content (<15 ppm) as well as unfractionated REE patterns from La to Lu (La/Lu_n 1-1.5 X chondrite) suggest participation of the mantle. Similarly, in the ϵ^t_{Nd} - ϵ^t_{Sr} diagram (Fig. 12), the mafic samples plot close to the mantle reference field (Fig. 12). Abdel Rahman (1990) suggested that the gabbroic magma is formed by partial melting of a mantle wedge previously hydrated by fluids released from a subducted oceanic crust.

The dioritic rocks have a calc-alkaline affinity and geochemical aspects of volcanic arc-lava. The field relationships and chemical and isotopic compositions of the diorites and gabbroic rocks suggest a petrogenetic link between these two rock types. The gabbroic rocks have the appropriate mineralogy, whole rock composition and isotopic signature to be a possible parental source for the dioritic rocks. However, least square calculations for major elements, together with the results of trace elements modelling obtained by Rayleigh equation do not give satisfactory results. Also, the increase of Sr with SiO_2 (Fig. 5), the negative correlation of CaO versus Sr and Ba (Figs. 7A and B, trend I) and the slight variation in compatible elements (*e.g.* V, Ni, and Cr) argue against crystal/melt fractionation. The chemical differences (for major, trace and REE) and isotopic similarity of the two rock types can be best explained by non-modal partial melting of the metagabbro to form the dioritic rocks.

A test of the partial-melting model for the diorite-quartzdiorite is based on conventional Sr, Ba, Rb and REE systematic. The most primitive gabbroid sample (sample No. 685) is used as an approximate initial source composition for the diorite. The concentration of Rb, Sr, Ba and REEs in the partial melts (F= 0.1-0.25) are calculated, using the batch melting equation (non-modal melting) of Shaw (1970):

$$C^i_l = C^i_o \ / D_o + F\,(1\text{-}P)$$

C^i_l and C^i_o are the concentrations of an element (i) in the melt and source respectively. D_o is the bulk distribution coefficient for the source assemblage, F is the fraction of melt, and P is the bulk distribution coefficient of the minerals (using their weight normative fraction) that enters the melt. The results and methods used in the calculations are given in Table 3. They refer to the evolu-

tion stage from the most primitive metagabbro (No. 685) to the least evolved diorite (No. 966) and the results point to a possibility that the diorites could have been derived by 10-15% melting of a basaltic source comparable in composition to the calc-alkaline metagabbro.

TABLE 3. Non-modal partial melting model *of the diorite rocks in the DIC.

	Parent composition no. 685	Estimated melt composition				Observed composition no. 966
		F # 0.10	F = 0.15	F = 0.20	F = 0.25	
La	5.20	8.40	8.02	7.70	7.40	8.90
Ce	15.30	21.00	20.20	19.40	18.80	22.40
Nd	9.80	8.50	8.40	8.30	8.20	11.70
Sm	3.80	2.61	2.60	2.60	2.59	3.20
Eu	1.40	0.85	0.88	0.90	0.93	0.90
Gd	3.30	2.07	2.07	2.08	2.08	3.20
Yb	2.60	2.26	2.24	2.22	2.20	1.60
Rb	11.00	80.00	59.90	47.70	39.00	27.00
Sr	182	284	289	297	301	463
Ba	82	487	387	322	275	406

* Proportions of phases present in the parent source (metagabbro) and the contributions of each phase to the melt are 0.4 clinopyroxene, 0.25 hornblende, 0.32 plagioclase, 0.02 magnetite, 0.01 apatite and .337 hornblende, .65 plagioclase, 0.01 magnetite, 0.003 apatite.

Degree of partial melting.

Petrogenesis of the felsic suite

Monzogranites

The DIC monzogranites belong to the calc-alkaline association (Figs. 4A and C) and have geochemical characteristics typical of I-type, arc-related granitoid (Figs. 6A&B). On the basis of field, geochemical and isotopic criteria, the origin of the monzogranites by fractionation from a basic or intermediate magma is unlikely as: (1) The monzogranite is too voluminous to be a direct fractionation product of the mafic-intermediate suite (gabbro-diorite). (2) The presence of a significant compositional gap in the major-and trace element composition (Fig. 5), particularly if we consider that the granodiorite is not a member of the fractionation series as discussed later. (3) The different REE patterns of the monzogranites from those of the mafic and intermediate rocks (Fig. 10) lend support that these rocks evolved from different sources and/or have different fractionation history. (4) The incompatible trace-element ratios such as Rb/Ba commonly shows no variation during fractional crystallization (Fig. 13), as ex-

pected for elements with similar partition coefficients during fractionation process. The increase of Rb/Ba from diorite to monzogranite (Fig. 13) further argues against fractionation of monzogranites from basaltic or dioritic magma.

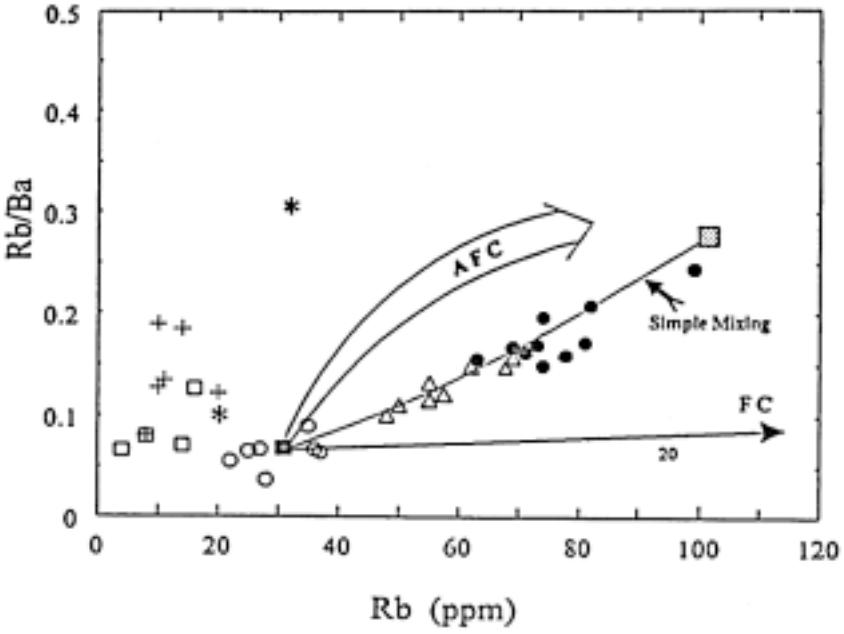

FIG. 13. Rb/Ba versus Rb diagram showing the effect of fractional crystallization (FC), assimilation-fractional crystallization (AFC) and simple mixing processes on the behavior of trace elements in the DIC. The arrow (FC) represents the fractionation trend calculated using Rayleigh formation law. The amounts of residual melt are also shown on the fractionation line. The arrow (AFC) represents the assumed general trend of assimilation-fractional crystallization. Note, the mafic rocks (gabbroic rocks) do not participate in the evolution of the granitoid rocks. Symbols as in Fig. 4.

In spite of these constraints, the abundance and behaviour of some trace elemenstill reflect the effect of some mineral fractionation. The DIC monzogranites are relatively LREE enriched with flat-shaped HREE (Gd-Yb) patterns. In acidic magmas, separation of appropriate proportions of hornblende and apatites is able to produce this effect without strong HREE fractionation. The large increase in HREE concentrations (Fig. 10) also need quartz crystallization in order to reduce the HREE bulk distribution coefficients. Moreover, strong negative Eu anomalies and depleted Sr are indicative of plagioclase fractionation.

An alternative model of assimilation-fractional crystallization (AFC) of a basic magma contaminated by metasedimentary country rocks can explain the

variation in the ϵ^{t}_{Nd} values of the monzogranites (*e.g.* DePaolo, 1981; Liew and McCulloch, 1985), but can not account for the homogeneity and low Sr isotopic compositions. The absence of crustal and wall rock xenoliths in the monzogranites argues against this model. However, the range in ϵ^{t}_{Nd} values in the calc-alkaline monzogranites may be due to a variable Sm/Nd ratios and perhaps variable residence time in the crust.

The isotopic and chemical data suggest that the plausible source of the Dubr-Igla monzogranites is likely to be an igneous protolith, calling for a predominant role of melting process within the crust (*cf.* Stern *et al.* 1984). As proposed for the genesis of complex acid-basic plutonic associations (Michard *et al.,* 1980; BenOthman *et al.* 1984; Bickle *et al.* 1989), the different granite magmas were assumed to be derived from partial melting of a heterogeneous crustal basement induced by injection of gabbro-diorite magmas from a mantle source. The nature of the lower-crust beneath the Nubian Shield is presently poorly understood. Recent studies on xenoliths of the disrupted lower continental crust of the Pan African Afro-Arabian shield from the Saudi Arabian (McGuire and Stern, 1993) and Zabargad island (Red Sea)(Lancelot and Bosch, 1991) suggest that the lower crust is dominated by metaigneous, mafic granulites and amphibolite. Dehydration melting of mafic lower crust to produce melt of granitic composition was previously described (Tepper *et al.* 1993; Rapp and Watson, 1995). The most appropriate mechanism suggests that the heat budget necessary to initiate melting is a mafic magma rising from the mantle wedge (Halliday *et al.* 1980; Whitney, 1988). This mafic magma will tend to partially underplate and pond at a major density discontinuity (the base of the lower crust) and begin to crystallize and differentiate to lower density (Hildreth and Moorbath, 1988). As the lower crust continues to heat, anatexis can begin over larger regions through dehydration reactions (Whitney, 1988).

A viable hypothesis to explain the chemical and isotopic features of the calc-alkaline monzogranites involves: 1) dehydration melting of a mafic metaigneous lower crust due to underplating by mantle-derived magma. 2) fractional crystallization of a crustal-derived primitive granitic magma to produce the monzogranites in the DIC. Geochemical and isotopic modelling has been applied using isotopic ratios versus elemental abundance and REE systematic (DePaolo, 1981; Powell, 1984). On the $^{87}Sr/^{86}Sri$ versus Sr diagram (Fig. 14), the composition of a melt (MC) derived by 30% partial melting of a lower crust (McGuire and Stern, 1993) was calculated using the batch melting equation of Shaw (1970). Partition coefficients (Kd values) used for calculations are reported in Table 4. The crustal-derived melt (MC) is further subjected to fractional crystallization (Fig. 14), with separation of K-feldspar (35%), plagioclase (30%), hornblende (5%), biotite (5%), and quartz (25%) and minor apatite. The

Dubr-Igla monzogranites, as shown in Fig. 14, can be formed by 60%-70% fractionation from a melt previously produced by 30% partial melting of the lower crust.

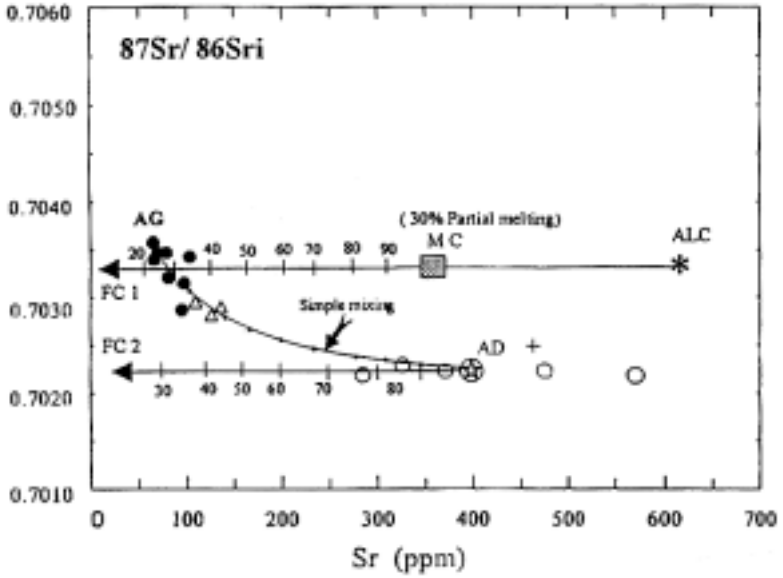

FIG. 14. Initial $^{87}Sr/^{86}Sr$ versus Sr (ppm) for modelling the DIC granitoid rocks. ALC represents the average composition of the Arabian-Nubian low crust (McGuire & Stern, 1993), MC stippled square is the melt composition formed after 30% partial melting of the ALC. The arrow FC-1 is the fractionation trend calculated using the crustal-derived melt (MC) as a source composition and the KD values given in Table (4). The arrow FC-2 is the fractionation trend calculated using the average diorite composition (AD) as a parent composition. The amounts of residual melts are indicated on each fractionation trend (FC-1 and FC-2). To model the origin of the granodiorite, a mixing hyberbola is also constructed using the mixing relationship given by Faure (1986). The average diorite composition, AD (star in circle) and the most differentiated monzogranite sample (AG) are used as the two end-member components. The mixing proportions are annotated on the mixing hyperbola, at 10%, by small dots. (see text for further details). Symbols as in Fig. 4.

To confirm the model in Fig. 14, using REE systematics, the source composition (lower crust) and degree of melting (F) adopted in the model of Fig. 14 are used in REE modeling. The REE contents of the source (Cº) and the modal mineralogy of the lower crust (70 % plagioclase; 15% orthopyroxene and 15% clinopyroxene) are taken from McGuire and Stern (1993). Using the composition of the melt derived by anatexis of the lower crust (MC) as a parent liquid, the concentration of REE in the residual liquids derived by 60-80 % fractionation (amount of separated crystals) are calculated using Rayleigh (1896) fractionation equation:

TABLE 4. REE and Trace element partition coefficients (Kds) *used for geochemical modelling of the DIC, Egypt.

Elements	Felsic rocks					Mafic-intermediate rocks					
	Hb**	Plag	Ksp	Bio.	Ap	Opx	Cpx	Hb	Plag	Mag	Ap
La	0.700	0.320	0.050	0.280	25.0	0.028	0.250	0.400	0.350	0.090	25.0
Ce	1.520	0.270	0.044	0.320	34.7	0.038	0.300	0.510	0.240	0.110	34.7
Nd	4.260	0.210	0.025	0.290	57.1	0.058	0.490	1.200	0.170	0.130	57.1
Sm	7.770	0.130	0.018	0.260	62.8	0.100	0.700	2.000	0.130	0.150	62.8
Eu	5.140	2.150	1.130	0.240	30.4	0.079	0.870	1.700	2.110	0.100	30.4
Gd	10.000	0.970	0.011	0.280	56.3	0.171	0.960	2.500	0.090	0.120	56.3
Yb	8.400	0.049	0.012	0.440	23.9	0.670	0.900	2.000	0.077	0.170	23.9
Rb	0.14	0.041	0.366	0.240		0.020	0.020	0.050	0.070		
Sr	0.220	4.400	9.400	0.120		0.020	0.080	0.230	1.800		
Ba	0.044	0.310	6.120	9.700		0.020	0.020	0.090	0.160		

* Sources of Kds values are from Arth (1976) and Hanson (1980).
**Cpx, Clinopyroxen; Opx, Orthopyroxen; Hb, Hornblende; Plag, Plagioclase; Ksp, K-feldspar; Bio, Biotite; Mag, Magnetite; Ap, Apatite.

$$C^{l} = C^{o}\ F^{D-1}$$

where C^l and C^o are the concentrations of elements in the residual and initial liquids respectively; *F,* amount of residual liquid and D is the bulk distribution coefficient. The results obtained by REE modeling (Fig. 15) indicate that the monzogranite represents a residual liquid left after 70-80% crystallization of plagioclase, K-feldspar, quartz, biotite and hornblende and minor apatite from crustal-derived magma. The results are also consistent with those obtained by isotopic modeling

Mafic-felsic magma interaction and origin of granodiorite

Various mafic-felsic magmas interaction (*e.g.* mingling, mixing, hybridization)(Eichelberger, 1978; Marshall and Sparks, 1984; Bacon, 1986; Bloomfield and Arculus, 1989) are now described by many authors in calc-alkaline plutonic environment (Reid *et al.* 1983; Frost and Mahood, 1987; Zorpi *et al.* 1989; Fernandez and Gasquet, 1994). Field and petrographic observations (Fig. 3), chemical and isotopic data (Figs. 5, 9, 13 and 14) leave no doubt that the granodiorites in the DIC are generated by magma mixing and variable degrees of hybridization. Comparable field relations were also described for the Tichka complex, Morocco (Fernandez and Gasquet, 1994); Gil-Màrquez complex, SW Spain (Castro *et al.* 1995) and orogenic granitoids of Northern Sardinia (Zorpi *et al.* 1989). Hassanen *et al.* (1996) has suggested that hybrid rocks (granodioritic composition), in Gabal Igla Ahmar (the southern part of DIC) is the result of mixing between acid magma (monzogranite) and diorite. The mafic (dio-

rite) and the felsic magmas (monzogranite) constitute the two major end-member components in the Dubr-Igla complex. Participation of these two end-members (diorite and monzogranite) on the genesis of granodiorite in the DIC is supported by the diagram Rb/Ba vs. Rb (Fig.13). The heterogeneous composition of the granodiorites is due to the varied proportion of each end-member contributed during the mixing or hybridization stage. In spite of the nature and intensity of interaction between the intermediate and acid, the granodiorite samples selected for chemical analyses and numerical modeling are those which have a rather homogeneous composition (*e.g.* containing only few xenoliths, no large grain size variation and no extreme enrichment or depletion in the incompatible elements). Reid *et al.* (1983) suggested that mafic inclusions in Sierra Nevada plutons represent chilled pillows of mafic magma and their fusion would produce granodiorites. A similar feature is also noticed in the DIC, where partial reactions of some mafic xenoliths in the felsic magma developed zoned-like xenoliths with diffused contacts (Fig. 3D).

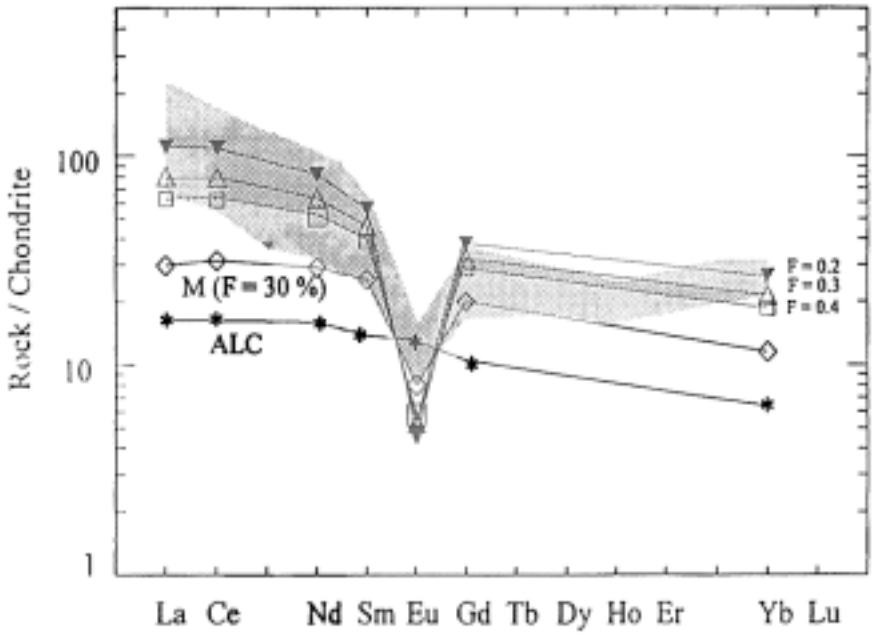

FIG. 15. REE-modelling of the DIC monzogranites. The calculated chondrite-normalized REE pattern of a melt-derived by 30% partial melting (MC) from the lower crust (ALC) is shown (McGuire & Stern, 1993). Also shown the calculated REE patterns of residual melts derived by 20%, 30% and 40% fractionation (F = 0.2, 0.3 and 0.4) from a 30% partial melt (MC). Distribution coefficients (Kds) are summarized in Table 4. The stippled field represents the composition of the DIC monzogranites.

On the $^{87}Sr/^{86}Sri$ versus Sr diagram (Fig. 14), a mixing curve is constructed using the mean compositions of diorite and monzogranite. The granodiorite samples plot close to the mixing hyperbola (Fig. 14), suggesting that the granodiorites are formed by about 20 to 30 % magma mixing of diorite and monzogranite. In order to calculate and confirm the possible range of mixing of each end-member component, a major element modeling is carried out using mass balance equations of LeMaitre (1981). Magma mixing is physically more efficient when the composition contrast, viscosity and density differences between the two mixed magmas are low enough to promote mixing (Frost and Mahood, 1987; Fernandez and Gasequte, 1994; Castro *et al.* 1995; Bateman, 1995). Accordingly, the most differentiated diorite sample (No. 972) and the less differentiated monzogranite (No. 680) are chosen as the two end-membecomponents. Table 5 shows the results of mixing calculation using two granodiorite samples (daughters) (Samples Nos. 652 and 651). The low r^2 values (sum of squares residuals) resulting from these calculations (1.86 and 1.66 respectively) confirm that magma mixing with a proportion from 17% up to 34% of dioritic end-member can account for major oxides variation of the granodiorite (Table 1). It is also in good agreement with the results of isotopic calculations. Although the chemical modeling is not unique, some rheological aspects must be considered. The thermal-rheological factors (*e.g.* temperature, viscosity, density, H^2O content and composition of the mafic and felsic magmas) put many constraints on the style and efficiency of mixing, volume and composition of the hybrids (*e.g.* SiO_2 content) (Fernandez and Gasquet, 1994). The rheological modeling proposed by Frost and Mahood (1987) indicates that hybrid rocks derived from mixing of mafic (basaltic) and felsic (granitic) magmas have small volumes and their SiO_2content does not exceed 63%. Also a large difference in the viscosity of the two end-members prohibits a homogeneous mixing of the two end-member components. In the DIC all the granodiorite samples contain more than 63% SiO_2.

These physical limitations on mixing in the DIC can be explained by the followings:

1 – Fractionation of the upper boundary layer of a mafic magma will produce a low density residual liquid that may eventually become lower in density than the overlying felsic magma (cf. Huppert *et al.* 1984). The buoyant residual liquid cause overturning and through mixing (Turner and Campbell, 1986; Fernandez and Gasquet, 1994; Bateman, 1995);

2 – Vesiculation of the mafic magma at shallow depth due to release of dissolved fluids and gases (Eichelberger, 1980; Thomas *et al.* 1993) would be sufficient to make the mafic magma buoyant relative to granitic magma;

3 – High shearing stresses rapidly and efficiently homogenize molten silicates (Kouchi and Sanagawa, 1983). Two major mechanisms could apply high

shearing stresses to coexisting magmas, namely, buoyant convection (Huppert *et al.* 1983) and tectonic shearing (Eichelbgerger, 1978; Whalen and Currie, 1984).

TABLE 5. Least square mixing calculations (LeMaitre, 1981) for the origin of granodiorite.

Oxides	Parent – 1 quartz-diorite no. 927	Parent – 2 monzogranite no. 680	Observed daughter – 1** no. 652	Estimated daughter – 1	Observed daughter – 2# no. 651	Estimated daughter – 2
SiO_2	61.28	73.71	68.22	68.27	71.52	71.63
TiO_2	0.57	0.25	0.41	0.39	0.27	0.30
Al_2O_3	15.62	13.31	15.22	14.32	14.67	13.70
Fe_2O_2	5.70	2.26	3.81	3.76	2.18	2.84
MnO	0.12	0.02	0.09	0.06	0.6	0.04
MgO	3.49	0.54	0.91	1.83	0.56	1.03
CaO	5.29	1.40	2.90	3.10	2.10	2.05
Na_2O	2.67	3.70	2.95	3.25	3.71	3.53
K_2O	2.30	3.31	2.61	2.87	3.04	3.14
P_2O_5	0.14	0.04	0.08	0.08	0.05	0.06
Parent – 1$				0.337		0.168
Parent – 2				0.663		0.832
r^{2}##				1.860		1.660

* Total iron as Fe_2O_3 $Proportions of the two end-member components (Parent – 1 & Parent – 2)
** Less differentiated granodiorite sample ## Sum of squares residuals
\# Most differentiated granodiorite sample

Conclusion

A combination of geochemical and Sr and Nd isotopic data are used to address the petrogenetic models for a calc-alkaline, composite batholith, the Dubr-Igla intrusive complex (DIC), in the Egyptian part of the Nubian Shield. The DIC has a wide compositional variation range from gabbro to granite. These rock associations belong to two distinct suites, the mafic-intermediate and felsic suites. The mafic-felsic rock associations from the two suites reveal field and chemical evidences of a complex magma interaction (mingling, mixing, heterogeneous to homogeneous hybridization). In terms of the abundance of major and trace elements, the gabbros and diorite-quartz diorite (mafic-intermediate suite) resemble island arc basalts related to subduction. Mineralogical and chemical characters (trace elements and REE) of granodiorite and monzogranite (felsic suite) indicate a close affinity to the I-type granite and affiliated to the post-orogenic granites.

The diorite-quartz diorite and monzogranite yield whole-rock Rb-Sr isochron ages of 704 ± 13 Ma and 644 ± 7 Ma respectively. The isotopic composition of

the mafic-intermediate suite (ϵ^{t}_{Nd} = 7.6-9.2 and initial $^{87}Sr/^{86}Sri$ ratio = 0.7022-0.7025) and depleted LILE and LREE represent potential fingerprint of a depleted mantle source. The granodiorite and monzogranites have low initial $^{87}Sr/^{86}Sr_i$ ratio (0.7025-0.7035) and relatively spread positive ϵ^{t}_{Nd} (3.4-5.2), which indicate that their protolith was most likely juvenile lower crust that had been separated from the mantle.

Geochemical and isotopic modeling indicate that the diorite is formed by 10%-15% partial melting of a basaltic source, similar in composition to the associated metagabbros. Dehydration melting (30%) of a mafic metaigneous lower crustal materials due to underplating by a mantle-derived basic magma followed by 70%-80% fractional crystallization of the crustal derived- primitive granitic melt yield the differentiated monzogranites in the DIC. This model for basaltic magmatic underplating as a primary cause of anatexis of the crust during the Late Proterozoic magmatic episode reconcile with abundance of an older mafic magma expressed by mantle-derived, mafic-intermediate rocks in the DIC and in the eastern Desert of Egypt. The granodiorite is the result of a variable extent of mafic-felsic magma interactions (mingling, mixing and hybridization). Least squares mixing calculations support the formation of the granodiorite rocks by a simple mixing of an approximate fraction of ca. 17% to 44% of the diorite with a less differentiated monzogranite.

Acknowledgements

The author greatly appreciates Dr. G. Matheis for providing facilities in the Technical University of Berlin. Ms. Angelika Brown and Mr. T. Domian are thanked for their technical assistance in XRF and ICP analyses. Dr. M. El Sayed is deeply thanked for doing the chemical and isotopic analyses at the Bergen University. Norway. Isotopic analysis at the Geological-Mineralogical Museum, Oslo, Norway could not be possible without the help of Dr. H. Harraz, Tanta University. The two journal reviewers Prof. A. El-Bouseily and H. Furnes are greatly acknowledged for their valuable suggestions, which improved the manuscript.

References

Abdel-Rahman, A. M. (1990) Petrogenesis of early orogenic diorites, tonalites and post-orogenic trondhjemites in the Nubian Shield. *J.Petrol.* **31:** 1285-1312.

Abdel Rahman, A. M. and **Doig, R.** (1978) The Rb-Sr geochronological evolution of the Ras Gharib segment of the Northern Nubian Shield. *J. Geol Soc. London* **144:** 577-586.

Abu ElEla, F. F. (1991) Bimodal volcanism of the Igla-Um Khariga metavolcanics, Eastern Desert, Egypt. *Egypt. Mineral.* **3:** 167-197.

Akaad, M. K. and **El-Ramly, M. F.** (1960) Geological history and classification of the basement rocks of the central eastern Desert of Egypt. *Geol. Surv. Egypt* **9:** 24-26.

Akaad, M. K. and **Essawy, M. A.** (1978) The metavolcanics around Bir Um Khariga eastern Desert, Egypt. *Bull. Fac. Science, Egypt* **18:** 118-129.

Akaad, M. K, Essawy, M. A. and **Shazly, A. G.** (1977) Two occurrences of the Igla Eliswid Formation in the Idfu-Marsa Alam and Qift-Quseir districts, Eastern Desert, *Egypt. Delta J. Sci.,* **1:** 21-42.

Allègre, C. J. and **BenOthman, D.** (1980) Nd-Sr isotopic relationship in granitoid rocks and development: a chemical approach to orogensis. *Nature* (London). **286:** 335-342.

Allègre, C. J., Hart, S. R. and Minster, **J. F.** (1983) Chemical structure and evolution of the mantle and continents determined by inversion of Nd and Sr isotopic data, II, Numerical experiments and discussions. *Earth Planet.Sci. Lett.,* **37:** 191-213.

Arth, J. G. (1976) Behaviour of trace elements during magmatic processes- a summary of theoretical models and their application. *J. Research. US Geol.* Surv., **4:** 41-47.

Bacon, C.R. (1986) Magmatic inclusions in silicic and intermediate volcanic rocks. *J. Geophys. Res.* **91:** 6091-6111.

Bacon, C. R. and **Metz, J.** (1984) Magmatic inclusions in rhyolites, contaminated basic compositional zonation beneath the Coso volcanic field, California. *Contrib. Mineral. Petrol.,* **85:** 346-365.

Bateman, R. (1995) The interplay between crystallization, replenishment and hybridization in large felsic magma chambers. *Earth-Sci. Reviews,* **39:** 91-106

Bennett, J. and **Mosley, P.** (1987) Tiered-tectonics and evolution, Eastern Desert, Egypt. In: **G. Matheis** and **H. Schandelmeier (Ed),** *Current Research In African Earth Science Balkema,* Rotterdam. pp. 79-82

BenOthman, D., Fourcade, S. and **Allègre, G. J.** (1984) Recycling processes in granite-granodiorite complex genesis: the Querigut case studied by Nd-Sr isotope systematics, *Earth Planet. Sci. Lett.,* **69:** 290-300.

Bickle, M.J., Bettenay, L.F., Chapman, H.J., Groves, D.I., McMaughton, N.I., Campbell, I.H. and **DeLaeter, J.R.** (1989) The age and origin of younger granitic plutons of the Shaw batholith in the Archean Pilbāra block, western Australia, *Contrib. Mineral. Petrol.* **101:** 361-376.

Bloomfield, A. L. and **Arculus, R. J.** (1989) Magma mixing in the San Francisco volcanic field, AZ, Petrogenesis of the O Leary Peak and Strawberry Crater volcanics. *Contrib. Mineral. Petrol.,* **102:** 429-453.

Castro, A., DeLeRosa, J. D., Fernández, C. and **Moreno-Ventas, I. (**1995) Unstable flow, mixing and magma-rock deformation in a deep-seated conduit: the Gill-Márqez complex, southwest Spain. *Geol. Rundsch.,* **84:** 359-374.

DePaolo, D. J. (1981) Trace element and isotopic effects of combined wallrock assimilation and fractional crystallization. *Earth Planet. Sci. Lett.,* **53:** 189-202.

Dias, G. and **Leterrier, J.** (1994) The genesis of felsic-mafic plutonic associations: a Sr and Nd isotopic study of Hercynian Braga Granitoid Massif (Northern Portugal). *Lithos,* **32:** 207-223.

Dixon, T. H. (1981) Age and chemical characteristics of some Pre-Pan-African rocks in the Egyptian Shield. *Precambrian Res.,* **14:** 119-133.

Duyverman, H. J., Harris, N. B. W. and **Hawksworth, C.J.** (1982) Crustal accretion in the Pan-African: Nd and Sr isotope evidence from the Arabian Shield. *Earth Planet. Sci. Lett.,* **59:** 15-326.

Eichelberger, J. G. (1978) Andesitic volcanism and crustal evolution. *Nature,* **275:** 21-27.

Eichelberger, J. G. (1980) Vesiculation of mafic magma during replenishment of silicic magma reservoirs. *Nature,* **288:** 446-450.

El-Gaby, S., List, F. K. and **Tehrani, R.** (1988) Geology, evolution and metallogenesis of the Pan-African belt in Egypt. In: **S. El-Gaby** and **O. R. Greiling (Ed),** *The Pan-African belt of NE-Africa and adjacent areas.* Vieweg & Braunschweig/ Wiesbaden, pp. 17-68.

El-Gaby, S., List, F. K., and **Tehrani, R.** (1990) The basement complex of the Eastern Desert and Sinai. *In:* **R. Said (Ed),** *The Geology of Egypt.* Balkema, Rotterdam, Brookfield, pp. 175-184.

El-Sayed, M. M. (1994) *Petrological and geochemical studies of Wadi El-Imera district, Eastern Desert,* Egypt. Ph. D. dissertation, Alexandria University, Egypt, 220pp.

El-Sharkawy, M. A. and **El-Bayoumi, R. M.** (1979) The Ophiolite of Wadi Ghadir area, Eastern Desert, *Egypt, Geol. Surv. Egypt,* **9:** 125-135.

Essawy, M. M. (1967) *Geology of the area around Bir Um Khariga, Eastern desert, Egypt,* (Ph. D. dissertation), Assiut University, Egypt, 446pp.

Faure, G. (1986*) Principles of isotope geology.* Wiley, New York, N. Y., second edition.

Fernandez, A. N. and. **Gaquet, D. R.** (1994) Relative rheological evolution of chemically contrasted coeval magmas: example of the Tichka plutonic complex (Morocco). *Contrib. Mineral. Petrol.,* **116:** 316-326.

Frost, T. P. and **Mahood, G. A.** (1987) Field, chemical and physical constraints on mafic-felsic magma interaction in the Lamarck Granodiorite, Sierra Nevada, California. *Geol. Soc. Am. Bull.,***99:** 272-291.

Furnes, H., El-Sayed, M., Khalil, S. O. and **Hassanen, M. A.** (1996) Pan-African magmatism in the Wadi El-Imra district, Central Eastern Desert, Egypt: geochemistry and tectonic environment. *Geol. Soc. London,* **153:** 705-718.

Gasquet, G., Leterrier, J., Mirini, Z. and **Vidal, P.** (1992) Petrogenesis of the Hercynian Tichka plutonic complex (western High Atlas, Morocco): Trace element and Rb-Sr and Sm-Nd isotopic constraints. *Earth Planet. Sci. Lett.,* **108:** 29-44.

Gillespie, J. G. and **Dixon, T. H.** (1983) Pb isotope systematics of some granitic rocks from the Egyptian Shield. *Precambrian. Res.,* **20:** 63-77.

Halliday, A. N., Stephens, W. E. and **Harmon, R. S.** (1980) Sr and O isotopic relationships in three zoned Caledonian granitic pluton, southern Uplands, Scotland: evidence for varied sources and hybridization of magmas.. *Geol. Soc. London,* **137:** 329-348.

Hanson, G. N. (1980) Rare earth elements in petrogenetic studies of igneous systems. *Ann. Review Earth Planet. Sci.* **8:** 371-406.

Hashad, A. M. (1980) Present status of geochronological data on the Egyptian basement complex. *Bull. Instit. Applied Geol., Jeddah,* **3:** 31-46.

Hashad, A. M., Sayyah, T. A., El-Kholy, S. B. and Youseff, A. (1972) Rb/Sr isotopic age determination of some basement Egyptian granites. *Egypt. J. Geol.* **16**(2): 269-281.

Hassan, M. A. and **Hashad, A. H.** (1990) Precambrian of Egypt. *In:* **R. Said (Ed),** *The geology of Egypt,* Balkema, Rotterdam, Brookfield, pp. 201-245.

Hassanen, M. A. (1985) *Petrology, geochemistry of ultramafic rocks in the eastern Desert of Egypt, with special reference to Fawakhir area.* Ph.D dissertation, Alexandria University, Egypt, 348pp.

Hassanen, M. A. and **Harraz, H. Z.** (1996) Geochemistry and Sr-and Nd-isotopic study on rare-metal-bearing granitic rocks, eastern Desert, Egypt. *Precambrian. Res.* **80:** 1-22

Hassanen, M. A., El-Nisr, S. A. and **Mohamed, F. H.** (1996) Geochemistry and petrogenesis of Pan African I-type granitoids at Gabal Igla Ahmr, eastern Desert, Egypt. *J. Afr. Earth Sci.,* **22**(1): 29-42.

Hassanen, M. A., Saad, N. A. and Khalefa, O. M. (1995) Geochemical aspects and origin of Tin-bearing granites in Egypt. *Acta Mineralogica-Petrographica Szeged,* **36:** 55-72

Hildreth, W. (1981) Gradients in Silicic magma chambers: Implications for lithospheric magmatism. *J. Geophys. Res.* **86:** 10153-1-10192.

Hildreth, W. and **Moorbath, S.** (1988) Crustal contribution to arc magmatism of central Chile. *Contrib. Mineral. Petrol.,* **98:** 455-489.

Huppert, H. E., Sparks, R. S. J. and **Turner, J. S.** (1983) Laboratory investigations of viscous effects in replenished magma chambers. *Earth Planet. Sci Lett.,* **65:** 377-381.

Huppert, H. E., Sparks, R. S. J. and **Turner, J. S.** (1984) Some effects of viscosity on dynamics of replenished magma chambers. *J. Volcanol. Geotherm. Res.,* **89:** 6857-6877.

Irvine, T. N. and **Baragar, W. R. A.** (19781) A guide to chemical classification of the common volcanic rocks. *Can. J. Earth Sc.,* **8:** 523-548.

Jackson, N. J. (1986) Petrogenesis and evolution of Arabian felsic plutonic rocks, *J. Afr. Earth Sci.* **4:** 47-59.

Kamel, O. A. and **Abdel Aal, A. Y.** (1987) K/Ar dating of some granitic rocks, Eastern Desert, Egypt. *In:* **G. Matheis** and **H. Schandelmeier (Ed),** *Current Research In African Earth Science* Balkema, Rotterdam. 91-94.

Kamel, O. A., El Bakry, A., El Mahallawi, M.,Balogh, K. and **Erva-Sos, E.** (1983) K/Ar dating of gabbro and granodiorite, Umm Rus area, Eastern Desert, *Egypt. 5th. Intern. Conf. Basement Tectonics,* Cairo, p. 31.

Klitzsch, F., List, F. K. and **Pöhlmann,** (1987) *The geological map of Egypt* 1: 500,000 - NG 36 SE Hamata-Conoco Coral. Institute für Angewandte Geodäsie, Berlin.

Kouchi, A. and **Sunagawa, A.** (1983) Mixing basaltic and dacitic magmas by forced convection. *Nature,* **304:** 527-528.

Lancelot, J. R. and **Bosch, D.** (1991) A Pan-African age foe the HP-HT granulite gneisses of Zabargad island: implications foe the early stages of the Red Sea rifting. *Earth Planet. Sci. Lett.* **107:** 539-549.

Langmuir, C. H., Vocke, R. D., Hanson, G. N. and **Hart, S. R.** (1978) A general mixing equation with applications to Icelandic basalts. *Earth Planet. Sci. Lett.,* **37:** 380-392.

LeMaitre, R. W. (1981) Genmix-a generalized petrological mixing program. *Computers and Geosciences* **7:** 229-247.

Liew, T. C. and **McCulloch, M. T.** (1985) Genesis of granitoid batholiths of Peninsular Malaysia and implications for models of crustal evolution. Evidence from a Nd-Sr isotopic and U-Pb zircon study. *Geochim. Cosmochim. Acta* **49:** 587-600.

Ludwig, K. R. (1991) Isoplot, a plotting and regression program for radiogenic isotopic data. *U.S. Geol. Surv. Open-file Report* **39:** 91-445.

Marshall, L. A. and **Sparks, R. S. J.** (1984) Origin of some mixed magma and net-veined ring intrusions. *Geol. Soc. London* **141:** 171-182.

Martin, H. (1986) Effect of steeper Archaic geothermal gradient on geochemistry of subduction zone magmatism. *Geology* **14:** 753-756.

McGuire, A. V. and **Stern, R. J.** (1993) Granulite xenoliths from western Saudi Arabia: a lower crust of Late Precambrian Arabian-Nubian Shield. *Contrib. Mineral. Petrol.,* **114:** 395-408.

Meschede, M. (1986) A method of discriminating between different types of mid-ocean ridge basalts and continental tholeiites with Nb-Zr-Y diagram. *Chem. Geol.,* **56:** 207-218

Michard-Vitrac, A., Albarede. F., Dupuy, C. and **Taylor Jr, H. P.** (1980) The genesis of Variscan (Hercynian) plutonic rocks: igneous complex, Central Pyrenees (Spain). *Contrib. Mineral. Petrol.,* **72:** 57-72.

Mittlefehldt, D. W. (1983) The lower crust of northern Israel. *Israel Geol. Soc. Ann. Meeting,* 58-59.

Moghazi, A. (1994) *Geochemical and radiogenic isotope studies of some basement rocks at the Kid area, southeastern Sinai, Egypt* Ph.D. dissertation, Alexandria University, Egypt 377 p.

Mohamed, F. H. and **Hassanen, M, A.** (1996) Geochemical evolution of arc-related mafic plutonism in the Umm Naggat district, eastern Desert of Egypt. *J. Afr. Earth Sci.* **22(**3): 269-283.

Pearce, J. A., Harris, N. B. W. and **Tindle, A. G.** (1984) Trace element discrimination diagrams for the tectonic setting interpretation of granitic rocks. *J. Petrol.* **25:** 956-983.

Pin, C. and **Carme, F.** (1987) A Sm-Nd isotopic study of 500 Ma old oceanic crust in the Variscan belt of western Europe: the Chamrousse ophiolite complex, Western Alps (France), *Contrib. Mineral. Petrol ,* **96:** 406-413.

Powell, R. (1984) Inversion of the assimilation and fractional crystallization (AFC) equations characterization of contaminants from isotope and trace element relationships in volcanic suite. *Geol. Soc. London* **141:** 447-452.

Rapp, R. P. and **Watson, E. B.** (1995) Dehydramelting of metabasalt at 8-32 kbar: Implications for continental growth and crust-mantle recycling. *J. Petrol.,* **36:** 891-931.

Rayleigh, J. W. S. (1896) Theoretical considerations respecting the separation of gases by diffusion and similar processes. *Phil. Magazine* **42:** 77-107.

Reid, J.B., Evanc, O.C. and **Fates, D.G.** (1983) Magma mixing in granitic rocks of the central Sierra Nevada, California, *Earth Planet. Sci. Lett.* **66:** 2433-2461.

Rice, A. H. N., Sakek, M. F. and **Rashwan, A. A.** (1993) Igneous and structural relations in the Pan-African Hammamat Group, Igla basin, Egypt. In: **U. Thorweihe** and **H. Schandelmeier (Ed)** *Geoscientific Research in Northeast Africa.* Balkema, Rotterdam, pp. 35-39.

Ringwood, A. E. (1975) *Composition and petrology of the Earth's mantle.* McGraw-Hill, New York p. 618.

Rogers, J. J. W. and **Greenberg, J. K.** (1990) Late orogenic, and anorogenic granites distinction by major-element and trace element chemistry and possible origins. *J. Geol.,* **98:** 291-309

Rushmer, T. (1991) Partial melting of two amphibolites: contrasting experimental results under fluid absent conditions. *Contrib. Mineral. Petrol.,* **107:** 41-59.

Saunders, A. D. and **Tarney, J.** (1979) The geochemistry of basalts from East Scotia Sea Spreading center in the East Scotia Sea. *Geochim. Cosmochim. Acta* **43:** 555-572.

Shaw, D. M. (1970) Trace element fractionation during anatexis.*Geochim. Cosmochim. Acta* **34:** 237-243.

Stanek, K. P., Phol, P., Li, Z. and **Shedit, G.** (1993) Rare-metal province central eastern Desert, Egypt-, I, Tectonic setting of magmatism In: **U. Thorweihe** and **H. Schandelmeier (Ed)**, *Geoscientific Research in Northeast Africa,* Balkema, Rotterdam, 477-482.

Stern, R. J. and **Hedge, C. E.** (1985) Geochronological and isotopic constraints on Late recambrian crustal evolution in the Eastern Desert of Egypt. *Am. J. Sci.,* **285:** 97-127.

Stern, R. J. and **Kröner, A.** (1993) Late Precambrian crustal evolution in NE Sudan: Isotopic and geochemical constraints. *J. Geol.,* **101:** 555-57.

Sun, S. S. (1982) Chemical composition and origin of the earth primitive mantle. *Geochim. Cosmochim. Acta,* **46:** 179-192.

Takla, M. A., Basta, E. Z. and **Fawazi, E.** (1981) Characterization of the older and younger gabbros of Egypt. *Delta J. Sci.,* **5:** 279-314.

Taylor, R. P., Strong, D. F. and **Kean, B. F. (**1980) The Topsails igneous complex: Silurian and Devonian peralkaline magmatism in western Newfoundland. *Can. J. Earth Sci.,* **17:** 425-439.

Tepper, J. H., Nelson, B. K., Bergantz, G. W. and **Irving, A.** J. (1993) Petrology of Chilliwack batholith, New York Cascades, Washington: generation of calc-alkaline granitoids by melting of mafic lower crust with variable water fugacity. *Contrib. Mineral. Petrol.,* **113:** 333-351.

Thomas, N., Tait, S. and **Koyaguchi, T.** (1993) Mixing of stratified liquids by the motion of gas bubbles: applications to magma mixing. *Earth Planet. Sci. Lett.,* **115:** 161-176.

Turner, J. S. and **Campbell, I. H.** (1986) Convection and mixing in magma chambers. *Earth-Sci. Rev.,* **23:** 255-352.

Walsh, J. N., Buckley, F. and **Baker, J.** (1981) The simultaneous determination of the rare-earth elements in the rocks using inductively coupled plasma source spectrometry. *Chem. Geol.*, **33:** 141-152.

Whalen, J. B. and **Currie, K. L.** (1984) The Topsails igneous terran, eastern Newfoundland: evidence for mixing. *Contrib. Mineral. Petrol.,* **87:** 319-327.

Whalen, J. B., Currie, K. L. and **Chappell, B. W.** (1987) A-type granites: Geochemical characteristic discrimination and petrogenesis. *Contrib. Mineral. Petrol.,* **95:** 407-419.

White, W. and **Patchett, J.** (1984) Hf-Nd-Sr isotopes and incompatible element abundances in island arcs: implications for magma origins and crust-mantle evolution. *Earth Planet. Sci. Lett.,* **67:** 167-185.

Whitney, J. A. (1988) The origin of granite: the role and source of water in the evolution of granitic magmas. *Geol. Soc. Am. Bull.,* **100:** 1886-1897.

Wolf, M. B. and **Wyllie, P. J.** (1994) Dehydration-melting of amphibolite at 10 kbar: the effects of temperature and time. *Contrib. Mineral. Petrol.,* **115:** *369-383.*

Wyllie, P. J., Cox, K. G. and **Biggar, G. M.** (1962) The habit of apatite in synthetic systems and igneous rocks. *J. Petrol.,* **3:** 328-243.

Zorpi, M. J., Coulon, C., Orsini, J. B. and **Cocirta, C.** (1989) Magma mingling, zoning and emplacement in calc-granitoid plutons. *Tectonophysics* **157:** 315-329.

دراسة جيوكيميائية ونظائرية للروبيديوم – استرنشيوم والسماريوم – نيوديميوم لمعقد دوبر – عجلة المتداخل بمصر : مثال لصهارات قاعدية – حمضية متمازجة

محمد عبد السميع حسنين

كلية علوم الأرض ، جامعة الملك عبد لعزيز ، جـــدة – المملكة العربية السعودية

المستخلص . يمثل معقد دوبر – عجلة المتداخل باثوليت مركب في معقد المصرية من صخور الحمى الأفريقي . وهو يمثل كتلة تركيبية مرفوعة تشتمل على تعدد صخري يتراوح من الجابرو إلى الجرانيت . هذه الصخور تنتمي إلى مجموعتين مميزتين وهما مجموعة الجابرو – دايوريت ومجموعة الجرانودايوريت – المنزوجرانيت . صخور الجابرو – دايوريت لها نزعة كلس قلوية مع انخفاض في محتوى عناصر الصوديوم والبوتاسيوم والأتريوم والروبيديوم بالإضافة إلى تفارق بسيط لعناصر الأرض النادرة . صخور بعد التجيل والممثلة بالجرانيت ، الجرانودايوريت والمونزوجرانيت ذات طبيعة كلس قوية وتتميز هذه الصخور بكونها ميتا الومينية إلى فوق الومينية مع إثراء في العناصر الليثوفية ذات الأيونات الكبيرة وشحيحة في العناصر ذات القوى المجالية العالية (HFS) .

لقد أعطت متساويات الزمن للروبيوديوم – استرنشيوم لكل من صخور المنزوجرانيت والدايوريت – كوارتز دايوريت في معقد دوبر – عجلة أعمار ٦٤٤ ± ٧ و ٧٠٤ ± ١٣ مليون سنة على التوالي . كما أن صخور الدايوريت تبين مدى محدود لكل من ابسلون النيوديميوم (٦,٧– ٨,٥) ونسبة استرنشيوم ٨٧/ استرنشيوم ٨٦ الابتدائية (٠,٧٠٢٢– ٠,٧٠٢٥) . هذا التركيب النظائري والمحتوى الشحيح لكل من العناصر الليثوفية ذات الأيونات الكبيرة وعناصر الأرض النادرة والنسبة المنخفضة في الروبيديوم/ استرنشيوم تثبت أن هذه الصخور قد نشأت وتطورت من وشاح شحيح كما وجد أن صخور الجرانودايوريت والمنزوجرانيت تحتوي

على نسبة استرنشيوم ٨٧/ استرنشيوم ٨٦ ابتدائية منخفضة (٠,٧٢٠٥ - ٠,٧٠٣٥) وانتشار موجب لابسلون نيودميوم (٤,٣-٢,٥) والتي تشير إلى أن مصدرها إما الوشاح أو القشرة السفلية النارية والتي قد انفصلت وتطورت من الوشاح .

الأنموذج العددي ونتائج كل من العناصر الأرضية النادرة والنظائر تشير إلى أن صخور معقد دوبر - عجلة قد تكونت من عمليات بتروجينية معقدة كما يلي :

١- الدايوريت - كوارتز دايوريت قد تكون من ١٠٪ - ١٥٪ انصهار جزئي لمصدر بازلتي ناتج من الوشاح ومشابه في التركيب لصخور الجابرو .

٢- الافتراض الذي يشرح السمات الكيميائية والنظائرية للمنزوجرانيت تتضمن : أ - انصهار جزئي (٣٠٪) للقشرة السفلية القاعدية نتيجة لتداخل مجما ناتجة من الوشاح . ب - تبلور جزئي لـ ٧٠٪-٨٠٪ من صهير جرانيتي أولى ناتج من القشرة الأرضية ليعطي المنزوجرانيت المتفارق في معقد دوبر - عجلة .

٣- الجرانو دايوريت يظهر كثير من الأدلة التي تشير إلى أنه تكون من تفاعل مجما مافية وأخرى فلسية . كما أن اختبارات وحسابات المزج باستخدام العناصر الشحيحة والأساسية تؤكد تكون صخور الجرانودايوريت بعملية مزج بسيط يتراوح من ١٥٪ إلى ٥٠٪ بين الدايوريت والمنزوجرانيت الأقل تفارق .